M 2015

U.PORTO

INSTITUTO DE CIÊNCIAS BIOMÉDICAS ABEL SALAZAR
UNIVERSIDADE DO PORTO

Ferritin Expression in Breast Cancer Infiltrating Lymphocytes

Evaluation of Biological Significance and Modulation by HLA-A*03 and HFE

LUCIANA REIS LEITE
DISSERTAÇÃO DE MESTRADO APRESENTADA
AO INSTITUTO DE CIÊNCIAS BIOMÉDICAS ABEL SALAZAR
DA UNIVERSIDADE DO PORTO EM
ONCOLOGIA MOLECULAR

Luciana Reis Leite

Ferritin Expression in Breast Cancer Infiltrating Lymphocytes

Evaluation of Biological Significance and Modulation
by HLA-A*03 and HFE

Dissertação de Candidatura ao grau de Mestre em Oncologia (Especialização em Oncologia Molecular) submetida ao Instituto de Ciências Biomédicas de Abel Salazar da Universidade do Porto.

Orientador – Professora Doutora Berta Martins da Silva
Categoria – Professora Associada
Afiliação – Instituto de Ciências Biomédicas Abel Salazar da Universidade do Porto

Co-orientador – Mestre Oriana Alexandra de Paixão Praças Marques
Categoria – Estudante de Doutoramento
Afiliação – Instituto de Ciências Biomédicas Abel Salazar da Universidade do Porto e Instituto de Biologia Molecular e Celular

“Por vezes sentimos que aquilo
que fazemos não é senão uma
gota de água no mar.
Mas o mar seria menor
se lhe faltasse uma gota.”

Madre Teresa de Calcutá

Este trabalho está inserido no projeto de Doutoramento em Patologia e Genética Molecular “Iron Homeostasis in Breast Cancer” da Mestre Oriana Alexandra de Paixão Praças Marques.

Parte dos resultados obtidos neste trabalho foram apresentados em formato de poster no “UMIB Summit 2015” realizado no Porto, de 24 a 25 de Setembro de 2015.

Embora uma dissertação de Mestrado seja, pela sua finalidade académica, um trabalho individual, existem contributos de natureza diversa que não podem e nem devem deixar de ser realçados. Por essa razão, desejo expressar os meus sinceros agradecimentos:

À Universidade do Porto, em particular ao Instituto de Ciências Biomédicas Abel Salazar (ICBAS), pela oportunidade que me deu de ingressar no Mestrado em Oncologia.

À Prof.ª Doutora Berta Martins da Silva que na qualidade de Diretora do Mestrado em Oncologia, Docente da cadeira de Imunologia e Cancro, Responsável pelo Laboratório de Imunogenética do ICBAS e, em especial, por ter aceite ser Orientadora do meu projeto me enriqueceu de forma inestimável com o seu rigor científico e metodológico. Agradeço por me transmitir o seu gosto pela Imunologia, o qual me fez querer redigir uma dissertação nessa área. Agradeço por fazer com que queira sempre mais e melhor. Agradeço todo o apoio transmitido nesta etapa fulcral de preparação para a minha futura carreira na investigação científica.

À Prof.ª Doutora Fátima Gärtner que na qualidade de Diretora do Departamento de Patologia e Imunologia Molecular do ICBAS me recebeu e autorizou a realização do meu projeto.

À Mestre Oriana Marques, que na qualidade de Co-orientadora do meu projeto, contribuiu para aquilo que sei hoje: deu-me a oportunidade de aprender e crescer cientificamente. Agradeço por me deixar fazer parte do seu trabalho de Doutoramento, por me ensinar a cada dia. Agradeço a disponibilidade, compreensão e ajuda inigualáveis, a paciência, as críticas, as correções e sugestões. Agradeço a palavra certa no momento certo.

Aos Docentes do 1º ano do Mestrado por estimularem o meu interesse pelo conhecimento e enriquecerem a minha formação científica.

Ao Prof. Doutor Carlos Lopes por atenciosamente ter feito a análise de todas as lâminas inseridas neste projeto.

Ao Prof. Doutor António Araújo, chefe do Serviço de Oncologia do Hospital de Santo António – Centro Hospitalar do Porto, que foi determinante na realização deste projeto, agradeço-lhe toda a disponibilidade demonstrada, recetividade e apoio. À Enfermeira Fátima do Hospital Santo António – Centro Hospitalar do Porto – pela ajuda na colheita das amostras de sangue às doentes.

À Prof.ª Doutora Graça Porto pela possibilidade que me deu de aprofundar os meus conhecimentos na semana dedicada ao Ferro, integrada no Programa Doutoral GABBA.

À Doutora Paula Faustino do Instituto Nacional de Saúde Dr. Ricardo Jorge por ter colaborado na genotipagem do HFE.

Às Doentes que voluntariamente aceitaram cooperar no meu projeto.

À Dra. Alexandra Rêma e à Dra. Fátima Faria pelo tempo precioso despendido em prol das minhas lâminas e pela simpatia com que sempre me receberam no laboratório.

À Dra. Ana Canadas pela prestimosa colaboração e espírito de entreajuda em momentos de maior "aflição".

Ao Mestre Arnaud Paula o tempo que graciosamente despendeu na recolha de dados oncológicos.

À Mestre Sandra Brás pela disponibilidade e prontidão. A sua colaboração foi sem dúvida uma mais-valia para a execução do projeto. Agradeço as suas palavras amigáveis e força transmitidas. Às Mestres Andreia Bettencourt, Bárbara Leal, Cláudia Carvalho, Daniela Boleixa e Dina Lopes por de uma forma, ou de outra, terem feito parte desta etapa. Agradeço também à Encarnação a sua boa disposição e simpatia diárias.

À Ana Rosa pelo apoio e paciência nos momentos de insegurança. Agradeço por ser a melhor colega de mestrado de sempre e por ter partilhado comigo este último ano. Ao Berto pela boa disposição, alegria e piadas constantes que me deixaram sem palavras em alguns momentos, contribuindo para que cada dia fosse melhor que o anterior. Agradeço também à Rita a amizade, o apoio prestado e a convivência diária.

À Mari, que mesmo estando longe fisicamente, me transmitiu a força e a coragem necessárias para permanecer na luta nos momentos mais delicados.

A todos os meus Amigos e Familiares por toda a energia e ânimo que me transmitiram para que conseguisse alcançar os meus objetivos.

Ao meu pequenino e querido Irmão David, que nunca me fez desejar ser filha única. Agradeço-lhe por preencher a minha vida de uma forma inexplicável e por estar sempre a torcer por mim. A Mi gosta muito de ti.

Aos meus Pais por todo o apoio, motivação, disponibilidade, paciência, suporte e confiança que depositaram em mim durante todo o meu percurso académico, assim como na minha formação pessoal. Agradeço-te Mamã por aturares as minhas casmurrices e os meus dramas. Agradeço-te Papá pela calma e tranquilidade transmitidas. Agradeço aos dois os valores que me transmitiram. Agradeço por me ensinarem a acreditar nas minhas capacidades e por me darem sempre amor e carinho. Agradeço por serem os Melhores Pais do Mundo! A vocês dedico este meu trabalho.

Por fim, agradeço a Deus por me amparar e dar força interior.

Introduction: Breast cancer development and progression are associated with a deregulation of iron homeostasis, as revealed by differences in the expression of several iron-related proteins. One of such proteins is ferritin, whose increased tissue levels have been consistently associated with breast cancer risk, severity and recurrence. Previous studies demonstrated that breast cancer infiltrating macrophages secrete mitogenic ferritin that stimulates the proliferation of breast cancer epithelial cells independently of its iron content. Our group has demonstrated that ferritin synthesis is also increased in breast cancer infiltrating lymphocytes. Accumulating evidence suggested that ferritin secretion could also be associated with the HLA-A*03 allele and HFE polymorphisms. The main objective of this project was to verify if a certain immune-profile was associated with an increased expression of ferritin in breast cancer infiltrating lymphocytes. Additionally, we analyzed if ferritin expression in breast cancer epithelial cells and lymphocytes was associated with clinicopathological variables of breast cancer progression and behaviour.

Methodology: Ferritin expression in breast epithelial cells and lymphocytes, and total CD4, CD8 and $CD4^+FoxP3^+$ T-cell numbers were assessed by immunohistochemistry in a total of 134 samples from tissue microarray blocks. The median ferritin expression in the epithelium and lymphocytic infiltrate was evaluated by a semi-quantitative method, considering the stained area and its intensity. The median number of total lymphocytes was assessed in 5 High-Power Fields (400x). Hemosiderin deposits in epithelial and stromal inflammatory cells were detected with the DAB-enhanced Perls' staining method. DNA extraction was performed from Formalin Fixed, Paraffin-embedded (FFPE) blocks and/or peripheral blood. HFE polymorphisms (C282Y and H63D) and HLA-A*03 genotyping were evaluated by Polymerase Chain Reaction (PCR).

Results: We confirmed that median ferritin expression was decreased in epithelial cells from carcinoma samples, but increased in infiltrating lymphocytes. These carcinoma samples were characterized by higher median numbers of $CD4^+$, $CD8^+$ and $CD4^+FoxP3^+$T-cells. Surprisingly the proportion of CD4/CD8 T-cells was not associated with an increased ferritin expression in lymphocytes. However, the FoxP3/CD4 ratio was positively correlated with the median ferritin expression in lymphocytes. In stromal inflammatory cells, the presence of hemosiderin deposits was associated with the median ferritin expression in epithelial cells and not in lymphocytes. In relation to clinicopathological variables, invasive ductal carcinoma (IDC) estrogen receptor (ER)

positive cases presented a significantly higher median ferritin. In ductal carcinoma *in situ* (DCIS) samples, the median number of total lymphocytes was significantly higher in hormone receptor negative cases. $CD4^+$ T-lymphocyte median numbers were significantly higher in ER negative, progesterone receptor (PR) negative and Human Epidermal Growth Factor 2 (HER-2) positive cases, in DCIS samples. A higher median number of $CD8^+$ and $CD4^+FoxP3^+$T-cells was observed in ER negative DCIS cases.

Conclusions: Our group has previously demonstrated that macrophages and lymphocytes present an "iron-donor" phenotype, as observed by its higher ferroportin 1 (Fpn1) expression in breast cancer tissue. However, evidences from other studies suggest that ferritin secretion, particularly by macrophages, may constitute an alternative route of iron delivery. The fact that ferritin expression in lymphocytes was not correlated with iron accumulation in stromal inflammatory cells may indicate a similar mechanism, not associated with ferritin's classical role as an iron storage protein. In fact, the "iron-donor" phenotype of tumor-infiltrating lymphocytes may play an important role in the tumor microenvironment, through the local regulation of iron homeostasis and potentially contributing to tumor nutrition.

Keywords: *Breast cancer; ferritin; stromal inflammatory cells; lymphocytes; regulatory T-cells; HLA-A*03 allele; HFE polymorphisms.*

Introdução: O desenvolvimento e progressão do cancro da mama estão associados com uma desregulada homeostasia do ferro, visível pela expressão alterada de proteínas associadas ao ferro. Uma dessas proteínas é a ferritina, cujos níveis aumentados têm sido consistentemente associados ao risco, severidade e recorrência do cancro da mama. Estudos anteriores demonstraram que os macrófagos presentes no microambiente tumoral da mama secretam ferritina mitogénica, estimulando a proliferação das células tumorais da mama independentemente do seu conteúdo em ferro. O nosso grupo demonstrou que em contexto de carcinoma da mama, a síntese de ferritina também se encontra elevada no infiltrado linfocitário. Está também documentado que a secreção de ferritina pode estar associada à presença do alelo HLA-A*03 e aos polimorfismos do gene do HFE. O principal objetivo deste projeto foi verificar se um certo "perfil imunológico" estaria associado com uma expressão aumentada de ferritina no infiltrado linfocitário do cancro da mama. Mais ainda, analisamos se a expressão de ferritina nas células epiteliais e nos linfócitos estava associada com variáveis clinicopatológicas referentes à progressão do cancro da mama.

Metodologia: A expressão de ferritina nas células epiteliais da mama e nos linfócitos, bem como número total de células T ($CD4^+$, $CD8^+$ e $CD4^+FoxP3^+$) foram quantificados por imunohistoquímica num total de 134 amostras de blocos de *tissue microarrays*. A expressão mediana de ferritina no epitélio e no infiltrado linfocitário foi avaliada através de um método semi-quantitativo, considerando a área com marcação e a sua intensidade. O número total mediano de linfócitos foi avaliado em 5 *High-Power Fields* (400x). A presença de depósitos de hemosiderina nas células epiteliais e do estroma foi detetada pelo método de coloração *DAB-enhanced Perls*. A extração de DNA foi realizada a partir de blocos de parafina e/ou sangue periférico. Os polimorfismos do gene HFE (C282Y e H63D) e a genotipagem do HLA-A*03 foram avaliados por *Polymerase Chain Reaction*.

Resultados: No nosso estudo, confirmou-se uma diminuída expressão mediana de ferritina nas células epiteliais em amostras de carcinoma, mas aumentada no infiltrado linfocitário. As amostras de carcinoma foram caracterizadas por um elevado número mediano de células T ($CD4^+$, $CD8^+$ e $CD4^+FoxP3^+$). Surpreendentemente, a proporção de linfócitos CD4/CD8 não foi associada com uma aumentada expressão de ferritina nos linfócitos. No entanto, o ratio FoxP3/CD4 foi positivamente correlacionado com a

expressão mediana de ferritina nos linfócitos. Nas células inflamatórias do estroma, a presença de depósitos de hemosiderina foi associada com a expressão mediana de ferritina nas células epiteliais, mas não nos linfócitos. Relativamente às variáveis clinicopatológicas, a expressão mediana de ferritina foi significativamente elevada em amostras de carcinomas ductais invasores positivas para os recetores de estrogénio. Nas amostras de carcinomas ductais *in situ*, o número mediano total de linfócitos foi significativamente elevado em casos que apresentaram negatividade para os recetores hormonais. Por sua vez, o número mediano de linfócitos T $CD4^+$ foi significativamente elevado em lesões *in situ* que apresentaram amplificação do HER-2 e negatividade para os recetores hormonais. O número mediado de células T ($CD8^+$ e $CD4^+FoxP3^+$) foi significativamente elevado em lesões *in situ* com negatividade para o recetores de estrogénio.

Conclusões: Anteriormente, o nosso grupo demonstrou que, no tecido de carcinoma da mama, os macrófagos e os linfócitos apresentam um fenótipo de exportação de ferro, visível pela expressão aumentada de ferroportina 1. No entanto, evidências provenientes de outros estudos sugerem que a secreção de ferritina, particularmente pelos macrófagos, pode constituir um papel alternativo de entrega de ferro. O facto da expressão de ferritina nos linfócitos não estar correlacionada com a acumulação de ferro nas células do estroma inflamatório sugere um mecanismo similar, não associado com o papel clássico da ferritina como armazenadora de ferro. De facto, o fenótipo de exportação de ferro do infiltrado linfocitário pode desempenhar um papel importante no microambiente tumoral, através da regulação da homeostasia do ferro, potencialmente contribuindo para a nutrição tumoral.

Palavras-chave: *Cancro da mama; ferritina; células inflamatórias do estroma; linfócitos; células T-reguladoras; alelo HLA-A*03; polimorfismos do HFE.*

% – Percentage

3,3'-DAB-4-HCl – 3,3'-Diaminobenzidine Tetrahydrochloride

AB buffer – Alcohol Buffer

APC – Adenomatous Polyposis Coli

APES – 3-aminopropyltriethoxysilane

Bp – Base Pairs

CD – Cluster of Differentiation

cf. – Confer

Corr coeff. – Correlation coefficient

DAB – 3,3-diaminobenzidinetrahydrochloride

DCIS – Ductal Carcinoma *in situ*

DMT1 – Divalent Metal Transporter 1

DNA – Deoxyribonucleic Acid

dNTP – Deoxynucleotide Triphosphate

EB buffer – Elution Buffer

EDTA – Ethylenediaminetetraacetic Acid

EGFR – Epidermal Growth Factor Receptor

ER – Estrogen Receptor

Fe^{2+} – Ferrous Iron

Fe^{3+} – Ferric Iron

Fe-S Cluster – Iron-Sulfer Cluster

FFPE – Formalin Fixed, Paraffin-embedded

FoxP3 – Factor Forkhead Box P3

FPN 1 – Ferroportin 1

Ft – Ferritin

g – Gram

H – Heavy

H&E – Hematoxylin & Eosin

H_2O_2 – Hydrogen Peroxide

HER-2 – Human Epidermal Growth Factor 2

HFP – High-Power Fields

HH – Hereditary Hemochromatosis

HLA – Human Leukocyte Antigen

IDC – Invasive Ductal Carcinoma

IFN-γ – Interferon-gamma

IHC – Immunohistochemistry

IREs – Iron-Responsive Elements

IRP1 – Iron-regulatory Protein 1

IRP2 – Iron-regulatory Protein 2

IRPs – Iron-regulatory Proteins

L – Light

LIP – Labile Iron Pool

M – Molarity

mg – Milligram

$MgCl_2$ – Magnesium Chloride

MHC-I – Major Histocompatibility Complex I

mL – Milliliter

NaCl – Sodium Chloride

NaN_3 – Sodium Azide

ºC – Degree Celsius

OH^- – Hydroxyl Radical

OS – Overall Survival

PB buffer – Pre-elution Buffer

PCR – Polymerase Chain Reaction

PR – Permanent Red

PR – Progesterone Receptor

RCLB – Red Cell Lysis Buffer

RFLP – Restriction Fragment Length Polymorphism

RFS – Relapse Free Survival

ROS – Reactive Oxygen Species

Rpm – Rotations per minute

RR – Ribonucleotide Reductase

SDS – Sodium Dodecyl Sulfate

SNP – Single Nucleotide Polymorphism

SPSS – Statistical Package for Social Science

TAE – Tris-acetate-EDTA

TBS – Tris-buffered saline

TE – Tris-EDTA

TE-2 – Tris-EDTA 2X

Tf – Transferrin

TfR1 – Transferrin Receptor 1

TMA – Tissue Microarray

Treg – Regulatory T-Cell

U/µL – U/microliter

UTR - Untranslated Region

V – Volt

WB buffer – Washing Buffer

µL – Microliter

µm – Micrometer

µM – Micromolar

CHAPTER I

INTRODUCTION

1. Iron Homeostasis

Iron is the most abundant transition metal in the human body and it is the fourth most abundant element in the Earth's crust [1, 2]. This element is essential for life as it plays an important role in normal cell growth, cell function and proliferation [3, 4].

Iron acts as a cofactor within the active site of key enzymes involved in important biochemical pathways [5], allowing it to act as an electron donor and acceptor during its conversion amid ferric (Fe^{3+}) and ferrous (Fe^{2+}) oxidation states [2].

Iron is also vital for the regulation of DNA synthesis and consequently cell cycle control, given that the enzyme accountable for the synthesis of desoxyribonucleotides, ribonucleotide reductase (RR), is iron dependent [6-8].

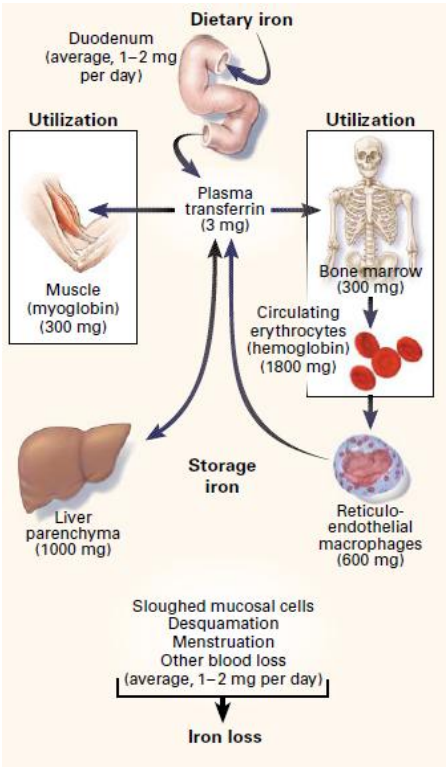

Figure 1 – Body iron distribution in human adults. Adapted from: [7].

However, iron in excess is toxic [5], due to the deleterious effects of reactive oxygen species (ROS), like the hydroxyl radical ($OH^{\cdot}$) which is produced via the Fenton and Haber-Weiss reactions [2, 5]. Free iron is able to react with unsaturated lipids, enhancing the lipid peroxidation process [9]. All of these oxidative reactions may result in the impairment of cellular functions and lead to damaged cells, tissues, and organs [10].

Although the majority of organisms have mechanisms to control iron acquisition, storage and export, there has been growing body of evidence relating a deregulation of iron homeostasis and a variety of diseases, including cancer, inflammatory and neurodegenerative diseases [11].

1.1. Systemic Iron Homeostasis

Once iron is vital for a variety of cellular processes, its stability must be maintained to prevent toxicity [5, 8, 12]. The regulation of iron is achieved through its absorption, utilization, storage and export [13], since there humans have no physiologic pathway for iron excretion [7].

The majority of iron is acquired from the diet (approximately 1-2 milligram per day), in the form of non-heme or heme iron [2, 7]. Dietary iron is absorbed by duodenal enterocytes through passage by their apical and basolateral membranes [7]. The divalent metal transporter 1 (DMT1) is responsible for the transport of inorganic iron across the apical enterocyte membrane [5], after reduction of its ferric (Fe^{3+}) form [2]. Following iron entrance in the enterocyte, it may be stored inside ferritin (Ft), an iron storage protein, or it may be transferred across the basolateral membrane by ferroportin 1 (FPN1) [2, 5].

Systemic iron homeostasis requires controlled intestinal iron absorption, utilization of iron for erythropoiesis and storage of iron by hepatocytes and reticuloendothelial macrophages [7, 14]. Systemic iron fluxes are regulated by the hepatic peptide hormone hepcidin [15]. Hepcidin is mostly produced by hepatocytes and disseminated in the blood bound to α2-macroglobulin [16]. Other cell types and organs also synthesize it, although to a much lesser extent [17]. Hepcidin was shown to have ability to down-modulate the cellular expression of FPN1 in enterocytes, macrophages and hepatocytes, which express high levels of FPN1 [15, 17]. This hormone binds FPN1, causing its internalization, ubiquitination and degradation [18, 19]. As a result, less iron is exported from enterocytes and from iron stores in hepatocytes and macrophages into the bloodstream [20]. The expression of hepcidin is regulated by a range of stimuli, like iron availability, inflammation, erythropoietic demand, hypoxia and endocrine signals [17].

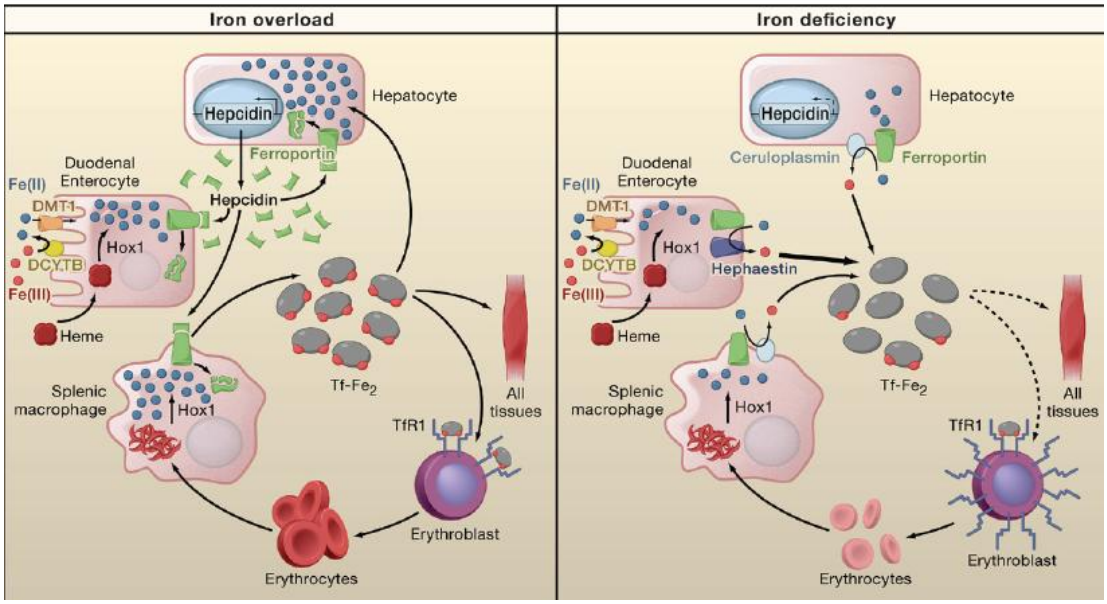

Figure 2 – Regulation of systemic iron homeostasis by hepcidin. Adapted from: [8].

1.2. Cellular Iron Homeostasis

Once in circulation, iron is included in transferrin (Tf) [2]. Tf transports iron in the bloodstream, keeping it in a soluble, non-toxic, form, and delivers iron to the required organs [5, 21, 22].

On the cell surface, Tf binds to the transferrin receptor 1 (TfR1) and this complex is then internalized into an endosome, via receptor-mediated endocytosis [5, 21]. Then, a pH proton pump-mediated reduction happens (pH ~ 5,5), enhancing iron release due to conformational changes in the Tf-TfR1 complex [23, 24]. Following iron release, the metal enters on the labile iron pool (LIP), which behaves as a metabolic source of iron [25]. LIP is a generic term used to describe labile iron in the cell as a whole [25]. Iron from the cytoplasmatic LIP that is not utilized for metalation reactions or exported can be targeted to ferritin [8, 26].

A finely control of iron uptake, storage and export is obtained by the regulation of proteins at the post-transcriptional level via the intracellular iron concentration [8]. Iron-regulatory proteins 1 and 2 (IRP1 and IRP2) are mRNA binding molecules identified as key iron sensors, forming a post-transcriptional regulatory network through which iron homeostasis is controlled [3, 12]. These two IRPs binds to iron-responsive elements (IREs) located in the 5'- or 3'-untranslated regions (UTR) of their mRNAs [27]. These IRE-containing mRNAs include TfR1, Ft and FPN1 [12]. The binding

between IRPs and IREs is regulated by intracellular iron levels and enables cells to quickly adjust concentrations of available cytosolic iron [27, 28].

In iron-depleted cells, IRPs binds to their target IREs [28]. When an IRP binds to the IRE located in the 5'-UTR of Ft mRNA, it leads to the blockade of its translation, for example, decreasing Ft abundance, in order to promote iron availability [29]. Conversely, the interaction between IRPs and the five IREs in TfR1 3'-UTR mRNA stabilizes it, favoring its translation [30]. In cells that are iron replete, IRPs do not have affinity for the IREs, leading to TfR1 mRNA degradation and Ft mRNA translation [28]. In these circumstances, cells inhibit further iron uptake by the transferrin receptor and, at the same time, promote storage of excess cellular iron in ferritin [2].

1.2.1. Ferritin

Approximately 25-30% of the iron in the adult human body is found bound to ferritin, which incorporates iron in a non-toxic and bioavailable form [1, 31, 32].

Ferritin is a protein, mainly localized in the cytoplasm, which is expressed in all cells [12, 14, 33], and composed by 24 subunits of 21kDa H- (heavy) and 19kDa L- (light) types [14, 34]. The expression of both functionally and genetically distinct ferritin subunits vary, depending on the cell type and in response to stimuli, including inflammation or infection [32-35]. H-ferritin possesses enzymatic activity: oxidizes ferrous iron (Fe^{2+}) into ferric iron (Fe^{3+}), required for the incorporation of iron into holo-ferritin [36, 37]; L-ferritin lacks enzymatic activity, not contributing to iron uptake, but to the stable storage of iron in the ferritin core [8, 14, 37, 38].

Additionally to its intracellular form, ferritin is also an abundant protein in circulation, termed serum ferritin [37]. Its immunologic reactivity and molecular size are similar to the ferritin extracted from the liver, but it shows low levels of iron even in patients with iron overload [37, 39]. Serum ferritin level is a decisive indicator of the body's iron stores, wherein patients with an iron overload disease presented higher levels of it [40, 41]. However, previous data proposed that intracellular ferritin would be a more valuable diagnostic marker than serum ferritin [42].

The storage of iron within ferritin prevents ROS formation, protecting the cell from oxidative damage [5], and defends cancer cells from cell death [35]. So, cells can lock up their excess iron in a redox inactive form to avoid iron-mediated cell and tissue damage [8, 12].

1.2.1.1. Ferritin Synthesis by T-lymphocytes

Stromal inflammatory cells from breast tissue can induce variations in the breast microenvironment, during malignant transformation [43]. Particularly, earlier results by Maria de Sousa's group showed that human T-lymphocytes synthesize and secrete ferritin [44].

Another study performed by Pollack and colleagues observed that individual variation in ferritin secretion by activated mononuclear cells is associated with the HLA-A locus [45]. Their study constituted the first evidence demonstrating that cells from individuals expressing HLA-A*03 antigen presented a reduced ferritin secretion *in vitro*, compared to those without A3 [45].

1.2.2. HFE

The HFE gene was discovered in 1996 by Feder and coworkers [46]. This gene is located on the short arm of chromosome 6 (6p21.3) [46, 47]. HFE is a major histocompatibility class I-like (MHC-I) molecule and associates with the class I light chain β2-microglobulin [46].

HFE was shown to interact with transferrin receptor 1 (TfR1) at a site that overlaps the transferrin binding domain, and to act as a negative regulator of iron absorption and uptake, through regulation of its binding partner – the TfR1 [8, 48, 49].

Previous studies have shown that HFE is the gene mutated in the large majority of Hereditary Hemochromatosis (HH) patients [14, 50, 51], a common genetic disorder of iron overload [51, 52]. Two polymorphisms, C282Y (the substitution of tyrosine for cysteine at position 282) and H63D (the substitution of aspartate for histidine at position 63), are particularly common among patients with HH [46]. The majority of HH patients are homozygous for the C282Y polymorphism in HFE [2, 53-55]. The C282Y polymorphism disrupts the correct folding of the α3 domain of the protein, interfering with its interaction with β2-microglobulin, and, consequently, abolishing the cell surface expression of the molecule [53]. The second missense polymorphism associated with hemochromatosis, H63D, does reach the cell surface and forms a stable complex with transferrin, being responsible for the loss of the ability of the HFE protein to increase the $K_{\text{cell association}}$ for transferrin [49, 56].

2. Breast Cancer

Breast cancer is the second most common cancer in the world and the most frequent in women [57]. Its incidence has been increasing over the years, especially in older women [58]. However, with a better and more efficient diagnostic method and improved therapies, the death rate associated to breast cancer has been diminishing over the decades [59, 60].

The majority of breast cancers are carcinomas once they occur from breast epithelial elements [59]. Non-carcinomatous breast cancers are uncommon and are originated in the connective tissue of the breast [58].

Ductal carcinomas can be divided in two major types: *in situ* and invasive carcinomas [59]. When the tumor remains confined to their ductal epithelium, without invasion, it is considered an *in situ* carcinoma [59]. In contrast, when the tumor invades the epithelial border it is called an invasive ductal or lobular carcinoma, with a higher metastatic potential [59].

Breast cancer can also be classified into sporadic or hereditary type, according to its origin [61]. The sporadic type is the most common malignancy of the breast and is associated with somatic genetic alterations [62]. On the other hand, the hereditary type is associated with germline mutations [63].

The aetiology of breast cancer is multifactorial: the breast tumor type and degree of aggressiveness can be affected by age, gender, family and personal history, radiation, microenvironment and diet factors [58]. The incidence of this malignancy increases with age, doubling about 10 years until menopause when the rate of increase slows significantly [64]. However, the curve decreases by the ages 75 to 80 [64]. The gender is considered the greatest risk factor: breast cancer is 100 times more frequent in women than in men [59]. In breast malignancy, obesity is related with an increased risk of recurrence and decreased survival [65]. Data about the smoking status is inconsistent, but a recent report has suggested an important role of active smoking in breast cancer development, predominantly with long-term heavy smoking and smoking initiation at an early age [66]. Alcohol consumption has also been linked to increased blood levels of estrogen, improving the risk of breast cancer development [67]. On the other hand, physical activity diminished its risk of development [65]. A diet low in folate, but rich in red or well-done meat, dairy and soy products are described as a potential cause of increased risk for breast cancer development [58, 68].

2.1. Immune System and Breast Cancer

Previous studies have shown that the immune response may play an important role in cancer progression [69-73]. The immune system may improve the emergence of primary tumors by reducing its immunogenicity and allowing tumor cells to escape immune recognition and destruction [74-76]. Despite tumor immunosurveillance, tumor cells must circumvent both innate and adaptive immunologic defenses in order to proliferate [71, 75]. So, the immune microenvironment in which the tumor develops may influence multiple parameters of the carcinogenic process [77].

Heterotypic interactions between diverse leukocyte populations often determine the outcome of immune responses in tissues [78], which were correlated with tumor grade, lymph node metastasis and overall survival (OS) of patients [79]. Particularly, in breast cancer, the immune microenvironment is also considered as a predictor of relapse free survival (RFS) and overall survival (OS) of patients [77], emphasizing the functional significance of specific leukocytes [80]. A variety of leukocytes have been found in breast cancer tissue, including $CD4^+$ and $CD8^+$ T-cells [80]. $CD4^+$ and $CD8^+$ T-lymphocytes recognize tumor antigens in the context of MHC class II and class I proteins, respectively [75].

$CD8^+$ T-lymphocytes are considered a crucial component of tumor specific cellular-adaptive immunity [70, 71, 81], exerting their antitumor activity [69]. $CD8^+$ T-cells produce interferon-gamma (IFN-γ) through interaction with tumor related antigens, potentially leading to tumoricidal activity by induction of apoptosis, or macrophage tumor killing activity, or both [82]. A variety of studies have reported that inflammation and $CD8^+$ T-lymphocyte infiltration in breast cancer are related with better survival of patients [35, 69, 71, 77, 83-85].

$CD4^+$ T-lymphocytes are vital controllers of immune responses and inflammatory diseases [86]. Earlier studies reported that these lymphocytes require interleukin-10 for their antitumor activity [87]. Human breast cancers containing leukocytic infiltrates dominated by $CD4^+$ T-lymphocytes, without significant $CD8^+$ T-cell infiltration, have a higher relative risk for metastasis and therefore, reduced overall survival (OS) [77, 88]. It was demonstrated that $CD4^+$ T-lymphocytes can promote metastasis by activating the Epidermal Growth Factor Receptor (EGFR) signaling pathway [88].

Regulatory T-cells (Tregs) have a key role in the maintenance of immune tolerance to both self- and harmless foreign antigens [89]. Tregs comprise a subpopulation of $CD4^+$ T-lymphocytes which play an essential role in inhibiting protective immune responses against tumors [75, 81, 90-93], including their ability to suppress a variety of immune cells (including CD4 and CD8 lymphocytes, dendritic cells, B cells and macrophages) and cytokine production [81, 91, 94-96]. Tumors may

facilitate the generation, activation, or function of immunosuppressive T-cell populations, such as Tregs [70, 75, 81, 93]. Their recruitment in the tumor microenvironment may enable malignant cells to escape from immunosurveillance [71, 90, 92-94].

The transcription factor forkhead box P3 (FoxP3) has been previously used to quantify Tregs, once it is known as the most specific marker of Treg [81, 90, 92, 96]. This transcription factor was also found to be localized in the nucleus of breast cancer cells [70, 90, 92, 93]. The identification of human Tregs is achieved through analysis of co-expression of CD4 and FoxP3, together with high expression of CD25, resulting in a $CD4^+/CD25^+/FoxP3^+$ activated phenotype [90, 92, 96].

The number of these tumor-associated Tregs was considered as a significant parameter for disease prognosis [94]. Elevated levels of Tregs were found in a variety of human cancers, including breast cancer [75, 90, 93, 94, 96], which was correlated with a poorer prognosis [70, 90, 92-94]. In invasive ductal carcinomas, Tregs are more frequently present, than in normal breast tissue, reinforcing that accumulation of Tregs represents a marker of breast cancer disease progression [94].

2.2. Iron Metabolism and Breast Cancer

The proliferation of normal cells is not feasible without the supply of adequate nutrients and oxygen to sustain cellular growth [97, 98]. The high levels of iron, required for the fast proliferation of neoplastic cells, have been recognized as a risk factor for cancer development [5, 12, 99]. In fact, several studies have found an association between the deregulation of mechanisms responsible to control iron homeostasis in the body and tumor growth, metastasis and high disease recurrence of a variety of cancers [1, 12, 38, 100, 101].

Breast cancer is no exception [100, 101]. Numerous studies showed that alterations in the expression of iron-associated proteins may clarify breast cancer cells' iron-deficient phenotype, characterized by an increased expression of iron importers and decreased expression of iron exporters [2, 4, 12, 102-104].

One of the most well known alterations in the iron metabolism of tumor cells is the up-regulation of TfR1 expression at the cell surface [105]. Cancer cells commonly express higher numbers of TfR1, than its normal counterparts, favoring iron uptake and consequently conferring a growth advantage to these cells [12, 102, 105-109]. It was proposed as a marker of poor prognosis in breast cancer [110].

The major Fe-transport protein in the plasma is Tf, as described above [101]. Tf behaves as a growth factor due to its iron-binding properties, making Tf crucial to cell proliferation and tumor growth in poorly vascularized areas [21, 111]. A previous study

described that Tf was produced by myoepithelial cells in normal ducts and around neoplastic ducts in carcinomas *in situ* [112].

Pinnix and colleagues highlighted the crucial role played by ferroportin 1 and hepcidin in the deregulation of iron homeostasis in breast cancer cells [4]. Their study revealed that ferroportin 1 protein levels were decreased in breast cancer epithelial cells compared to normal epithelial cells [4]. Regarding hepcidin expression, Zhang and colleagues observed an increase of its expression in breast cancer tissue [15]. These findings suggested that the breast cancer cells' "iron-deficient" phenotype is compatible with their proliferation status.

2.2.1. Ferritin and Breast Cancer

A link between ferritin and inflammatory conditions, as infections and cancer, has also been reported [2, 8, 12, 35, 101, 113].

In contrast with healthy individuals, several studies have reported a higher serum ferritin expression in patients with solid tumors, including breast cancer [42, 114-116]. These high levels of serum ferritin and also, an increased ferritin expression within breast tumors, were correlated with a poor clinical outcome, due to higher degrees of inflammation [12, 42, 114, 117-119].

The histological examination of expression and distribution of ferritin demonstrated a strong ferritin expression in epithelial ductal cells from normal breast tissue, a moderate to weak staining in breast cancer cells and a relatively strong staining in the tumor stroma [112, 119, 120].

Some reports have described an alteration in the subcellular distribution of ferritin [35, 121]. H-ferritin can be translocated to the nucleus to protect DNA from iron-mediated toxicity, once it is able to sequester iron in excess, favoring cancer cells survival [34, 35, 122]. In this way, Liu and colleagues emphasized the potential importance of subcellular localization of H-ferritin in breast cancer progression [35].

As described above, T-lymphocytes are able to synthesize ferritin [44, 45, 123]; however, recent *in vivo* studies have argued that serum ferritin is primarily derived from macrophages [124, 125]. In line with this information, Alkhateeb and colleagues not only proved that breast cancer-associated macrophages were capable of ferritin secretion, but also, extracellular ferritin enhances the proliferation of breast cancer cells lines, independently of its iron content [120]. Hence, Alkhateeb and colleagues speculated that the increase of serum ferritin in breast cancer patients, which was correlated with tumor stage [126, 127], could reflect an inflammatory state involving tumor-associated macrophages [120].

Thus, ferritin could act not only as the major iron storage protein, but also as an important regulator of the immune system playing a role in epithelial carcinogenic transformations, potentially enhancing an effective anti-tumor immune response [33, 35, 113, 128].

2.2.2. HFE and Breast Cancer

HFE gene is located in one of the most frequently amplified regions of chromosome 6p, which are involved in tumor development and progression [47, 129, 130].

HFE polymorphisms are able to modify iron stores by triggering overload of iron [2, 130, 131]. Moreover, the altered iron homeostasis that may cause iron accumulation, potentially contributed to tumor progression, behaviour and aggressiveness and was associated with an elevated risk for cancer development [132-135].

Beckman and colleagues performed the first study in order to investigate the association between HFE gene polymorphisms and breast cancer risk [136]. Their analysis was based on statistical evidence and suggested the existence of an interaction between HFE and Tfr alleles, which increased the cancer risk [136]. Subsequent investigations confirm that HFE gene polymorphisms might be associated with breast cancer risk [137].

Osborne and colleagues reported that the majority of C282Y homozygous eventually could develop an iron overload-related disease, once they presented higher serum ferritin [130]. These individuals have an elevated risk for breast cancer development compared with those who had no C282Y polymorphism [130]. Although C282Y heterozygous present an elevated serum ferritin and transferrin saturation level, compared to individuals without HFE polymorphisms, they had not an improved risk for breast cancer development [104, 138]. Nevertheless, Hunt and colleagues observed that most C282Y heterozygous did not exhibit abnormalities in body iron parameters [139].

Regarding the H63D polymorphism, some studies demonstrated that it was associated with breast cancer [140-142].

Actually, studies concerning the association of HFE polymorphisms and breast cancer risk have led to contradictory and inconclusive results [143], once there are studies that did not report an association [140, 144]. This suggests the existence of a population variability concerning HFE gene polymorphisms [145].

2.2.2.1. HFE and The Immune System

Growing evidence suggests a role for HFE in the immune system [51, 53]. HFE gene has been showed to be localized in a short region around the Human Leukocyte Antigen (HLA-A) locus [146]. In spite of the large physical distance between HFE and HLA, a linkage disequilibrium has been demonstrated between HLA-A and HFE gene polymorphisms [147]. The strong linkage disequilibrium between C282Y polymorphism and the extended haplotype containing the HLA-A*03 allele was *a posteriori* confirmed [46, 148].

As described above, HFE gene is mutated in the majority of patients with hereditary hemochromatosis [51]. These patients, with HFE polymorphisms, contain an irregular expression of MHC-I molecules and an altered class I antigen presentation pathway [149]. In addition, they present an altered peripheral $CD8^+$ T-cell pool and CD4-CD8 ratio [150, 151]. According to this information, a report suggested an important role of HLA-A*03 on the correlation between CD4-CD8 ratio and the severity of iron overload [52]. In fact, Porto and coworkers demonstrated that in the context of HLA-A*03, the relative proportions of $CD4^+$ and $CD8^+$ T-cells were significantly correlated with the amount of iron stores accumulated at the time of diagnosis, predisposing patients to a more severe illness [52]. A subsequent study performed by Maria de Sousa's group also suggested that the relative proportion of CD4/CD8 lymphocytes may be considered as a significant predictor and modifier of iron overload development [152]. As the HFE was described as a nonclassical MHC protein, they assumed that immunological system and iron metabolism are inseparable [152].

CHAPTER II

AIMS

The **major goal** of this project is to verify if a certain immune profile is related with a higher expression of ferritin in breast cancer infiltrating lymphocytes, and analyze if this is correlated with patient clinicopathological variables.

Others objectives:

1. To assess if the number of lymphocytes is correlated with ferritin expression;
2. To evaluate if the presence of nuclear ferritin is associated with ferritin expression;
3. To verify if hemosiderin deposits are associated with the type of lymphocytic profile and ferritin expression;
4. To investigate if ferritin expression by T-lymphocytes in breast tumors is associated with HLA-A and HFE genotypes;
5. To estimate if these relationships are associated to established clinicopathological variables, such as, hormone receptor status, tumor size and lymph node involvement.

CHAPTER III

MATERIAL AND METHODS

1. Breast Cancer Tissue Samples

A total of 120 cases, including 34 ductal carcinomas *in situ* (DCIS) and 54 invasive ductal carcinomas (IDC) from formalin fixed, paraffin-embedded (FFPE) breast samples were collected from the archives of the Pathology Service, at Centro Hospitalar do Porto (Porto, Hospital Centre, Porto). All of them were previously gathered for the PhD project in which this study is integrated and approved by the Centro Hospitalar do Porto Ethics Committee (Porto, Hospital Centre, Porto, Portugal). 32 reduction mammoplasty samples were also included, accounting as normal breast tissue.

All samples were considered as representative of primary breast tumors, assembled from women who were diagnosed between 2004 and 2009, and who weren't submitted to any neoadjuvant treatment.

The areas, diagnosis and classification of tumors were performed by a board certified pathologist according to the tumor classification criteria. He analyzed slides of 88 samples of primary tumors and 32 samples of reduction mammoplasty, with the purpose of selecting normal, *in situ* and invasive areas, whenever possible.

2. Construction of Tissue Microarrays

In 1998, Kononen and colleagues developed the tissue microarray (TMA) technology that allows researchers to sample up to 1000 tumors on one glass slide, which can be evaluated by fluorescence *in situ* hybridization or immunohistochemistry [153]. Small cylindrical cores are removed from formalin-fixed, paraffin-embedded tissue and placed in a matrix within a recipient paraffin block, according to a previous designed map. This high-throughput technique makes a fast examination of hundreds of patient samples by a pathologist feasible [154].

Comparing to whole sections, the staining of a few TMA sections reveals an advantage with respect to the reduction of laboratory reagents and technician time. Additionally, there is the benefit of reduced technical variability during the staining and interpretation process [154].

The most common disadvantage of TMA use is the short size of each tissue core – there is hesitation that due to tumor heterogeneity, biomarker scores obtained from small TMA cores will not exactly reflect scores obtained from whole tissue sections. There also exists a technical problem related with TMA studies, which is the tissue loss during sectioning, transfer and staining. The mixture of sampling errors during core extraction,

core loss during slide preparation and non-reactive cores leads to loss of biomarker data and an underestimation of the right incidence of a molecular indicator. This difficulty can be reduced by the extraction of several cores per source block [153, 154].

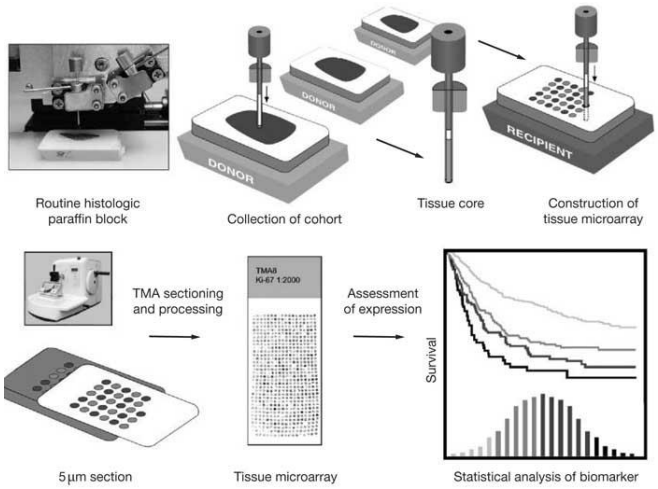

Figure 3 – Representative image of a TMA block construction. (Adapted from: http://www.nature.com/nrclinonc/journal/v1/n2/fig_tab/ncponc0046_F1.html).

So, we constructed tissue microarrays for screening a large number of tissue samples under similar experimental conditions. From the original paraffin blocks, a pathologist selected areas of interest. After this, we used an extractor to remove those areas of interest in paraffin-embedded tissues of normal and tumor samples, according to a previously stipulated map. After this, we placed it into a TMA receiver block.

Normal liver and lymph node samples were also inserted, for correct slide orientation of cores and internal positive controls for stainings.

3. Hematoxylin & Eosin Staining

Formalin-fixed, paraffin-embedded tissues used were sectioned with a microtome into 2 µm sections. Slides were de-waxed by placing them in xylene twice for 5 minutes each. Then, they were hydrated in a series of decreasing alcohol concentrations (100% - 90% - 75%) for at least 1 minute each, and finally washed under running water for 2 minutes.

Slides were stained with hematoxylin (Mayer's Hemalum Solution, Merck Millipore, Billevica, MA, USA) and then rinsed in running tap water for 5 minutes.

Slides were stained with eosin for at least 1 minute and were placed rapidly under water.

After a fast differentiation in absolute alcohol, they were sequentially dehydrated in 70%, 90% and absolute alcohol and 2 changes of xylene. Slides were then mounted with Entellan (Merck Millipore, Billerica, MA, USA).

A pathologist evaluated Hematoxylin & Eosin (H&E) staining slides under the light microscope in order to classify the lesion of each spot. The pathologist was blinded of diagnostic and clinical information regarding the original donor tissue when evaluating the lesion in each spot.

4. Perls' Prussian Blue Stainin

Perls' Prussian Blue staining was performed to evaluate hemosiderin deposits in breast samples. Hemosiderin is a degradation product of ferritin, which is an iron storage complex [155]. This information provides a qualitative estimative, based on the evaluation of the presence of iron deposits in epithelial and stromal inflammatory cells. An iron loaded liver was used as a positive control section to ensure that the reaction has occurred.

TMA blocks were sectioned with a microtome into 2 µm sections. Slides were left at 70ºC for 5 minutes and then, at 37ºC until further techniques. Slides were then dewaxed, deparaffinized and hydrated as described for the H&E protocol.

We mixed equal parts of hydrochloric acid (2%) and potassium ferrocyanide (2%) prepared immediately before use. Slides were immersed in this Butting's solution for 20 minutes, at 70ºC. Then, they were washed in distilled water and counterstained with nuclear fast red, for 4 minutes. Slides were dehydrated through 100% alcohol and were cleared in xylene. Finally, slides were mounted with Entellan (Merck Millipore, Billerica, MA, USA) mounting medium.

After this, Perls' staining slides were assessed under the light microscope to detect hemosiderin deposits, in the epithelial and stromal compartments. A score of 1 was attributed when at least one cell presented hemosiderin deposits and a score of 0 when no hemosiderin deposits were observed.

4.1 DAB-enhanced Perls' Prussian Blue Staining

Knowing that in a majority of tissues iron is present in a low concentration and the threshold of its detection using the Perls' method is hardly reached in epithelial cells [156], intensification with DAB can be executed to augment sensitivity [157]. All samples were stained with an increase in incubation times of 25%, as Van Duijn and colleagues explained [158].

TMA blocks were cut with a microtome into 4 µm sections and mounted in adhesive slides with 3-aminopropyltriethoxysilane (APES). Slides were left at 70ºC, for 5 minutes, to increase tissue adherence to the glass surface, and then, placed at 37ºC until further techniques. Slides were dewaxed, deparaffinized and hydrated as described for the H&E protocol. After this,

slides were stained with “freshly” prepared 1% potassium cyanide, in distilled water (pH inferior to 5,5), for 40 minutes. Slides were washed in distilled water. Subsequently, samples were treated in methanol containing 0,01 M NaN_3 and 0,3% hydrogen peroxide (H_2O_2) for 75 minutes and washed with 0,1 M phosphate buffer. For the intensification reaction, slides were incubated with a solution containing 0,025% 3,3'-diaminobenzidine tetrahydrochloride (3,3’-DAB-4HCl) and 0,005% H_2O_2, in a 0,1 M phosphate buffer, for 40 minutes. The reaction was stopped by rinsing in distilled water.

After this, tissues were counterstained with nuclear red, for 4 minutes, and slides were differentiated in absolute alcohol until a pink contrasting color was achieved. Slides with the stained samples were mounted with Entellan (Merck Millipore, Billerica, MA, USA).

As reported in Roschzttardz’s work [156], we used a negative control, by omitting the incubation with potassium ferrocyanide. No staining was observed in these samples, showing that staining was hemosiderin dependent and not due to peroxidase-catalyzed degradation of H_2O_2, inducing the polymerization of DAB. As performed in routine Perls’ staining, a positive control tissue was also added to the experiment.

5. Immunohistochemistry (IHC)

Immunohistochemistry was performed with ferritin, in order to evaluate its expression at the cellular and nuclear level in breast epithelial cells and in resident and infiltrating breast tissue lymphocytes. For ferritin, immunohistochemistry was performed on tissue microarrays sections with a rabbit polyclonal anti-human ferritin antibody (FT – 1/1000, Sigma-Aldrich, MO, USA). After testing dilutions in 5% TBS.BSA solution, we decided that 1:1000 dilution provided the best results.

Immunohistochemistry was also performed in order to characterize the lymphocytic infiltrate, using CD4, CD8 and FoxP3 markers.

This technique was conducted according to manufacturer’s details using the Novocastra Novolink Detection System (Leica Biosystems). This detection system is systematically used in the Department and has been giving consistent results over a range of antibodies. For each antibody, we used a positive control recommended by the antibody’s manufacter and a negative control, by omission of primary antibody.

Tissue microarrays were sectioned with a microtome into 2 µm sections.

For CD8, single-immunohistochemistry was performed on tissue microarray sections with the mouse monoclonal anti-human CD8 antibody (C8/144B, Cell Marque, CA, USA). First, we tested three different dilution factors (1:25, 1:50 and 1:100), as initially

recommended by the manufacturer. All dilutions were performed with 5% TBS.BSA solution. We opted on the 1:100 dilution as the optimum dilution factor to this antibody.

For CD4 and FoxP3, double-immunohistochemistry was performed on tissue microarray sections with a mouse monoclonal anti-human CD4 antibody (BC/1F6, Biocare Medical, Concord, USA), and a mouse monoclonal anti-human FoxP3 antibody (236A/E7, eBioscience, San Diego, USA).

First, we performed a single immunohistochemistry for each antibody (CD4 and FoxP3) to decide the optimum dilution factor and the best chromogen reaction. For the monoclonal CD4 antibody, we tested 1:25, 1:50 and 1:100 dilution factors. All dilutions were performed in Van Gogh Yellow solution, a diluent provided by the manufacturer. We decided 1:50 dilution as the optimum dilution factor for this antibody. Subsequently, we tested which would be the best chromogen reaction for the observation of $CD4^+$ T-lymphocytes. We used as chromogens DAB and permanent red (PR) (Permanent Red Chromogen Kit, Cell Marque, California, US). We chose DAB as the best chromogen to visualize $CD4^+$ T-lymphocyte numbers.

For the FoxP3 antibody, we tested 1:50, 1:100 and 1:200 dilution factors. All dilutions were performed in 5% TBS.BSA solution, as suggested by the manufacturer. We chose the 1:200 dilution as the best dilution factor. As for CD4, we also tested the most suitable chromogens to observe FoxP3 immunoreaction, and opted for PR.

After optimizing antibody dilutions, we tested the CD4 and FoxP3 double-immunohistochemistry protocol. We performed this technique in different slides including positive controls, ductal carcinomas *in situ* and invasive ductal carcinomas. With the double-immunohistochemistry protocol, this CD4 antibody did not allow obvious identification of lymphocytes, so, we decided to purchase a new rabbit polyclonal anti-human CD4 antibody (H-370, Santa Cruz Biotechnology, TX, USA).

Once again, we executed single immunohistochemistry in positive control slides to decide which would be the best dilution factor between 1:100, 1:250 and 1:500 for this new antibody. All dilutions were performed in 5% TBS.BSA solution, as suggested by the manufacturer. We opted for the 1:250 dilution factor.

After optimization of the dilution factor, we performed CD4 and FoxP3 double-immunohistochemistry protocol in different slides, including positive control, ductal carcinomas *in situ* and invasive ductal carcinomas to test the protocol. Given that, double immunohistochemistry with these antibodies did not allow a clear discrimination of $CD4^+$ and $CD4^+FoxP3^+$ T-cells. Considering this, we decided to perform simultaneous labeling for both antibodies, since CD4 is a membrane surface glycoprotein and FoxP3 a nuclear transcription factor.

5.1 Immunohistochemistry Protocol

TMA blocks were cut at 2 μm and mounted in adhesive slides with APES. Slides were left at 70ºC, for 5 minutes, and then, at 37ºC until further techniques.

5.1.1 Deparaffinization and Rehydratation

Slides were deparaffinized and hydrated as described in H&E protocol.

5.1.2 Antigen Retrieval

Antigen retrieval was then performed using Dako Target Retrieval Solution, at 10%, in distilled water.

Slides were placed in the plastic staining jar containing the previously prepared solution. Staining jar was then allocated in a water bath, at 100ºC, for 25 minutes. After this, slides were taken out of the water bath and allowed to cool at room temperature.

When the slides were in the water bath, the immunohistochemistry chamber was prepared. For this, absorbent paper was cut and placed in the bottom of the chamber and impregnated with TBS.

5.1.3 Endogenous Peroxidase Blockade

We delimited the TMA section in the slide with a hydrophobic pen (NovoPen, Novocastra, Leica Systems) to prevent waste of reagents by keeping liquids in tension.

In the immunohistochemistry chamber, slides were incubated with 3 drops of peroxidase block (Peroxidase Block, Novocastra Novolink Detection System, Leica Systems) for 5 minutes, at room temperature. Slides were rinsed twice in TBS, 5 minutes each.

5.1.4 Protein Block

We eliminated the excess of TBS from slides by placing them in absorbent paper. Slides were incubated with 3 drops of protein block (Protein Block, Novocastra Novolink Detection System) for 5 minutes, at room temperature. This was done to block any unspecific antigen-antibody reaction that may lead to background staining.

5.1.5 Incubation of Primary Antibody

We removed the excess of protein block reagent and we incubated each glass slide with 150 µL of primary antibody, at the respective dilutions. Slides were kept in the immunohistochemistry chamber, overnight, at 4ºC.

5.1.6 Incubation of Secondary Antibody

In the following day, slides were washed twice in TBS for 5 minutes each. 3 drops of secondary antibody (Post-primary, Novocastra Novolink Detection System) were placed on each slide for 30 minutes, in the immunohistochemistry chamber, at room temperature. They were washed in TBS twice for 5 minutes each.

5.1.7 Polymer

In order to eliminate the excess of the secondary antibody, slides were placed in the absorbent paper.

Slides were incubated with 3 drops of the polymer (Polymer, Novocastra Novolink Detection System), for 30 minutes, in the immunohistochemistry chamber, at room temperature. After this, slides were rinsed twice in TBS, 5 minutes each.

5.1.8 Chromogen Reaction/ Revelation

3,3-diaminobenzidinetrahydrochloride (DAB) is an example of a chromogen. DAB is an electron donor which upon being oxidized produces an insoluble colored product (brown end color). We prepared 50 µL of DAB for each 1000 µL of substrate buffer.

Each slide was incubated with 150 µL of DAB solution, until visible revelation occurred. After this, slides were placed in a container with water and placed under running water, for 10 minutes.

5.1.9 Counterstaining

Slides were counterstained with hematoxylin and placed under running water for 10 minutes.

5.1.10 Dehydration and Clearing

Slides were sequentially dehydrated in 70%, 90% and absolute alcohol, and 2 changes of xylene.

5.1.11 Mounting of Slides

Slides were removed from the xylene and they were mounted with Entellan. We pressed each slide carefully after placing the cover slip to get rid of any bubbles present.

They were quickly passed through xylene and cleaned, after which they were allowed to dry for microscopic examination.

5.2 Analysis of TMA Slides

The IHC analysis was performed by an experienced pathologist who was blinded to the clinico-pathologic data.

5.2.1 CD8 Scoring

TMA spots were analyzed in order to evaluate the number of T-cytotoxic lymphocytes, as assessed by the expression of CD8 marker in breast tissue leukocytic infiltrates.

To perform CD8 T-cell count in each spot, CD8 positive cells were calculated in 5 High-Power Fields (HFP) (400x), under the light microscope taking into account CD8 immunoreactivity, to distinguish T-cytotoxic lymphocytes of other cells. The values obtained from the 5 HPFs were added, in order to obtain the total spot count of $CD8^+$ T-lymphocytes.

5.2.2 CD4 and FoxP3 Scoring

TMA spots were analyzed in order to evaluate the number of T-helper lymphocytes and regulatory T-cells (a subpopulation of $CD4^+$ T-lymphocytes [81]), assessed by the expression of CD4 and/or FoxP3 markers. Correspondingly, TMA sections were evaluated for the presence of CD4 and FoxP3. For this, 5 HPFs (400x) were visualized and counted under the light microscope. Lymphocytes presenting single immunoreactivity for CD4 antibody, at the cell or cytoplasm, were considered $CD4^+$ T-cells, while lymphocytes presenting double immunoreactivity for CD4 and FoxP3 antibodies were considered regulatory T-cells (Figure 4).

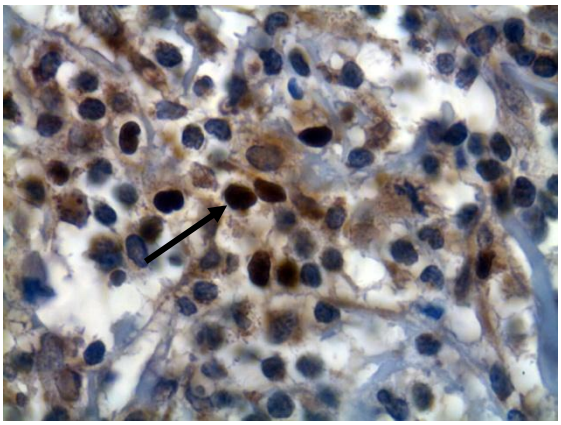

Figure 4 – Representative image of CD4 and regulatory T-cell identification (example of a double immunoreactivity for CD4 and FoxP3 antibodies signaled with an arrow), in an Invasive Ductal Carcinoma (IDC) sample (Magnification 1000x).

5.2.3 Ferritin Scoring

Regarding ferritin, we evaluated the localization (cytoplasm and/or nuclear), the immunostaining intensity and the area of epithelial and lymphocyte staining.

Nuclear ferritin expression was considered when more than 10% of the epithelial cells presented it.

6. DNA Extraction and PCR-RFLP

6.1 Biologic Samples

We selected one paraffin block from each patient, in order to perform HFE and HLA genotyping. All FFPE blocks used from Centro Hospitalar do Porto were the same collected for the PhD project in which this study is integrated.

The extraction of DNA was performed using the Ultraprep Tissue DNA kit (AHN Biotechnologie, Nordhausen, Germany). Using a clean, sharp microtome blade, we cut two 10 µm sections from each block. First cuts weren't used to avoid degraded DNA and contamination. The steel knife was cleaned between blocks with absolute ethanol to avoid DNA contamination.

When we performed HFE and HLA genotyping, this technique did not yield satisfactory results. Not only DNA was highly degraded in some blocks, not allowing HFE genotyping, nor HLA genotyping, given the high molecular weight of its PCR products. Hereupon, DNA extraction from peripheral blood was also performed.

As the blood collection was not inserted in the PhD project, we solicited an extended approval by the Centro Hospitalar do Porto Ethics Committee (Porto, Hospital Centre, Porto, Portugal) (2015.026(026-DEFI/024-CES)).

Peripheral blood was collected from women with breast cancer (diagnosis between 2004 and 2009), who were followed by the Oncology Service, at Centro Hospitalar do Porto. Blood was collected by venipuncture into tubes already prepared with EDTA.

6.2 Protocol of DNA Extraction from FFPE Blocks

TMA blocks were cut at 10 µm and slides were then left at 70ºC, for 5 minutes, and then, at 37ºC, until further techniques. Sections were deparaffinized 3 times in Ottix (DiaPath, Martinengo, Italy) (10 minutes each), and then, they were rehydrated through a descending series of alcohol (100%, 90% and 70%) to distilled water – 10 minutes each.

We used a 1,5 mL microcentrifuge tube for 2 slides of each case. To the 1,5 mL microcentrifuge tube, we added 250 µL of Pre-elution buffer (PB) and 20µL of proteinase K (both from Ultraprep Tissue DNA kit, AHN Biotechnologie, Nordhausen, Germany). Samples were scraped from the glass slides with the help of a pipette tip and placed in the corresponding eppendorf. We added the tissue sample and incubated, overnight, at 55ºC, in a thermomixer (300 rpm) with slight agitation.

In the next day, we removed all microcentrifuge tubes from the thermomixer and added 250 µL of Alcohol buffer (AB) to each tube and mix thoroughly by vortexing, for 15 seconds.

Samples were transferred to a new eppendorf with the kit column (500 µL). Tubes were then centrifuged for 1 minute, at 14500 rpm. The flow-through was discarded, without discarding the spin cup.

After adding 400 µL of Washing buffer (WB) solution, all microcentrifuge tubes were placed in a thermomixer for 1 minute, at 14500 rpm. The flow-through was discarded, without discarding the spin cup.

Columns were washed twice with 400 µL of 70% ethanol by centrifugation, at 14500 rpm, for 3 minutes. The flow-through was discarded without discarding the spin cup. After this, columns were transferred to a different eppendorf. 40 µL of Elution buffer (EB) solution, previously preheated at 70ºC, was added into each microcentrifuge tube and was incubated at room temperature, for 2 minutes. Tubes were centrifuged for 1 minute, at 14500 rpm, and columns were discarded.

6.3 Protocol of DNA Extraction from Peripheral Blood

Genomic DNA was isolated from leukocytes of peripheral blood using an altered “Salting Out” protocol, described in 1988, by Miller and colleagues [159]. This method, based on low solubility of proteins in the presence of high salt concentrations, allows for DNA extraction of high quality and quantity.

First, mononuclear cells (leukocytes) were separated by centrifuging blood samples, collected in EDTA tubes, at 3000 rpm, during 20 minutes. After this, we got two phases: one with erythrocytes, and a buffy coat – ring of leukocytes and a liquid phase (serum). We withdraw the plasma and the buffy coat (with some erythrocytes) to one Falcon tube of 50 mL, to which we added 50 mL of red cell lysis buffer (RCLB). The solution was homogenized and was incubated for 10 minutes, at room temperature. Subsequently, it was centrifuged at 2000 rpm, for 10 minutes, at 4ºC.

The supernatant (red blood cells and other cellular components) was discarded and the pellet of lymphocytes was washed with cold RCLB (4ºC), until we achieved a completely white pellet.

After this, we added 3,5 mL of Tris-EDTA 2X (TE-2) buffer, 200 µL of Sodium Dodecyl Sulfate (SDS) at 10% and 10 µL of proteinase K to the pellet. SDS solution is a detergent able to solubilize membrane proteins and, amongst with TE-2, enhance membrane lysis, promoting release of DNA by the precipitation of proteins [160].

After agitation, samples were incubated overnight, at 42ºC, allowing full cell digestion. After enzyme digestion, samples were transferred to a conical tube of 15 mL, to which was added 1 mL of sodium chloride (NaCl) (6M). This saline buffer leads to the precipitation of proteins and release of DNA.

Samples were vortexed and were slowly agitated by magnetic stirring, for 10 minutes, resulting in a white solution due to precipitation of proteins. After this, samples were centrifuged at 3000 rpm for 30 minutes, at 23ºC. Disregarding the protein content, the supernatant was transferred to a Falcon tube of 50 mL, to which we have added 20 mL of cold absolute ethanol (-20ºC). The ethanol solution removes water from the DNA molecule, forcing it to leave solution and precipitate.

Subsequently, DNA coils were washed with 5 mL of cold 70% ethanol (-20ºC), and were ressuspended in TE buffer solution, in an eppendorf tube of 2 mL. The volume of TE utilized to ressuspend the DNA was determined by empiric observation.

In the final step, tubes with DNA were disposed on a rotary shaker for, at least, 12 hours.

6.4 DNA Quantification

The DNA extracted from paraffin blocks and peripheral blood was quantified using a NanoDrop spectrophotometer (Saveen Werner, Malmö, Uppsala). Values of DNA concentration and the ratios between absorbances at 280 nm and 260 nm - that informs about DNA contamination of proteins ($A_{260/280}$) - and 260 nm and 230 nm ($A_{260/230}$) –, that indicates other contaminations (including salts or phenols) - were considered.

DNA was stored in a freezer, at -20ºC, until further usage.

6.5 Polymerase Chain Reaction (PCR)

PCR, first introduced by Mullins in 1986 [161], allows enzymatic *de novo* synthesis of a specific target DNA sequence. During repetitive cycles of denaturation, annealing of specific oligonucleotide primers and polymerase extension, the DNA sequence limited by the two primers is doubled in each cycle, mimicking the *in vivo* process of DNA replication.

The PCR reaction happens in three major phases [161]:

- **1st Phase -** DNA denaturation: this step involves high temperatures, around 95ºC, which separates the strands of the double helical DNA by breaking the hydrogen bonds forming single stranded DNA;
- **2nd Phase –** Annealing of specific primers: temperature is lowered, to facilitate the annealing of primers to the DNA template. The perfect temperature depends on the sequence of the oligonucleotide primers and their Guanine/Cytosine content;
- **3rd Phase –** Extension of DNA: it occurs at 72ºC, the ideal temperature for the polymerase activity. In this step, Taq polymerase extends the primers by adding the respectives deoxy nucleotide triphosphates (dNTPs).

6.5.1 HLA-A*03 Genotyping

Although we have tried to optimize the protocol of DNA extraction from FFPE blocks, it wasn't possible to perform because the DNA from FFPE blocks was highly degraded. Hence, we decided to perform DNA extraction from peripheral blood to detect

the presence of the HLA-A*03 allele. We prepared the mix for PCR reaction as described in Table 1.

Homemade-primers are optimized mixes of primers which are systematically used in the Immunogenetics Laboratory, Department of Pathology and Molecular Immunology, wherein, mixture 4 amplifies specifically HLA-A*0301 and HLA-A*0302, and the mixture 26 amplifies all HLA-A *locus*, except for the alleles 0201-19, 2301, 2402-12, 6801-3 and 6901.

Table 1 – Description of PCR reagents used for detection of HLA-A*03 allele.

Component	Initial Concentration	Final Concentration
Template DNA	Variable	≤ 1 µg DNA/50 µL
Green Bull Buffer [1] (Promega, Madison, WI USA)	1000x	1x
GoTaq DNA Polymerase (Promega, Madison, WI USA)	5 U/µL	5 U
$MgCl_2$ (Bioline, London, UK)	50 mM	1,45 mM
Forward/Reverse Primer	10 µM	5 µM
Bi-distilled Water (B. Braun Medical, Portugal)	Added to obtain the volume of 10 µL	

[1] **Green Bull Buffer:** 5x Green Buffer (final concentration: 1x); Bi-distilled water; $MgCl_2$ (25 mM) (final concentration: 2 mM), Mix dNTP's (25 mM) (final concentration: 200 µM).

The PCR program used for HLA-A amplification was the following: 2 minutes at 95ºC followed by 5 cycles of 10 seconds at 96ºC and 1 minute at 70ºC, followed by 15 cycles of 10 seconds at 96ºC, 30 seconds at 65ºC and 30 seconds at 72ºC, followed by 10 cycles of 10 seconds at 96ºC, 30 seconds at 60ºC and 30 seconds at 72ºC. At last, reaction was extended at 72ºC, for 10 minutes.

6.5.2 PCR-Restriction Fragment Length Polymorphism (PCR-RFLP)

Restriction fragment length polymorphism analysis of PCR-RFLP was performed to detect the C282Y (exon 4) and H63D (exon 2) polymorphisms in the HFE gene [46]. We prepared the mix for PCR reaction as described in Table 2.

Table 2 – Description of Multiplex PCR reagents used for amplification of the C282Y and H63D variant alleles.

Component	Volume/Reaction	Final Concentration
Template DNA	Variable	≤ 1 µg DNA/50 µL
2x Multiplex PCR Mastermix	25 µL	1x
Q-solution, 5x	5 µL	0,5x
HFE C282Y/H63D Forward Primer	100 µM	10 µM
HFE C282Y/H63D Reverse Primer	100 µM	10 µM
Bi-distilled Water	Variable	

For the HFE H63D polymorphism, the following forward and reverse primers' sequences were used, according to Feder's work [46]: 5'-ACA TGG TTA AGG CCT GTT GC-3' and 5'-GCC ACA TCT GGC TTA AAA TT-3', amplifying a 294 bp fragment. Sequences of primers used for detection of C282Y polymorphism were: forward primer, 5'-CAAGTGCCTCCTTTGGTGAAGGTGACACAT-3', and reverse primer, 5'-CTCAGGCACTCCTCTCAACC-3', amplifying a 343 bp fragment.

The PCR program used for H63D and C282Y amplification was the following: DNA suffered an initial activation step at 95ºC for 10 minutes. For 36 cycles, it was denatured at 94ºC for 30 seconds, annealed at 58ºC for 90 seconds, and extended for 90 seconds, at 72ºC. At last, reaction was extended at 72ºC, for 10 minutes.

6.6 Electrophoresis

Electrophoresis is supported by the principle that applying an electric field which force negative molecules, such as DNA, to migrate into the positive pole, through an agarose or polyacrylamide matrix [162]. This separates molecules by size, where smaller molecules move faster and migrate further through the gel [162].

First, we prepared an agarose medium gel, at 1,5%. In the erlenmeyer flask, we mixed 4,5 g of agarose with 300 mL of 1X TAE. Then, it was placed for 4 minutes, in a microwave, at full power.

After this, we added 25 µL of ethidium bromide (Sigma-Aldrich, MO, USA) to the erlenmeyer flask, and it was cautiously agitated, avoiding air bubbles in the agarose (GeneOn, Germany) solution. After the agarose solution cooled down, it was poured over a gel mold with the well combs in place. The agarose gel was completely solidified after 25-30 minutes. It was placed in the electrophoresis unit and was covered with 1xTAE, and the combs removed.

We added 5 µL of the amplicon to 2 µL of loading buffer, and this mix was loaded to the wells of the gel. In the first well of the gel, we placed a molecular weight ladder, with 100 bp, and then, the samples. The gel was run for approximately 1 hour, at approximately150 V. We transferred the electrophoresis gel to a chamber with ultraviolet light to analyze it.

For HFE gene polymorphisms (C282Y and H63D), we considered a successful amplification when a band with 294 bp and 343 bp, respectively, was identified in the gel.

For the HLA-A*03 allele, DNA was amplified by PCR with sequence-specific primers based on methods described previously [163]. Each reaction included an internal control, specific for the Adenomatous Polyposis Coli (APC) gene, which gives a 246 bp band indicating that the reaction works properly. For the HLA-A*03 locus tissue type, we considered that amplification occurs when two bands with 446 bp and 636 bp appear in the gel, for each specific reaction (Figure 5).

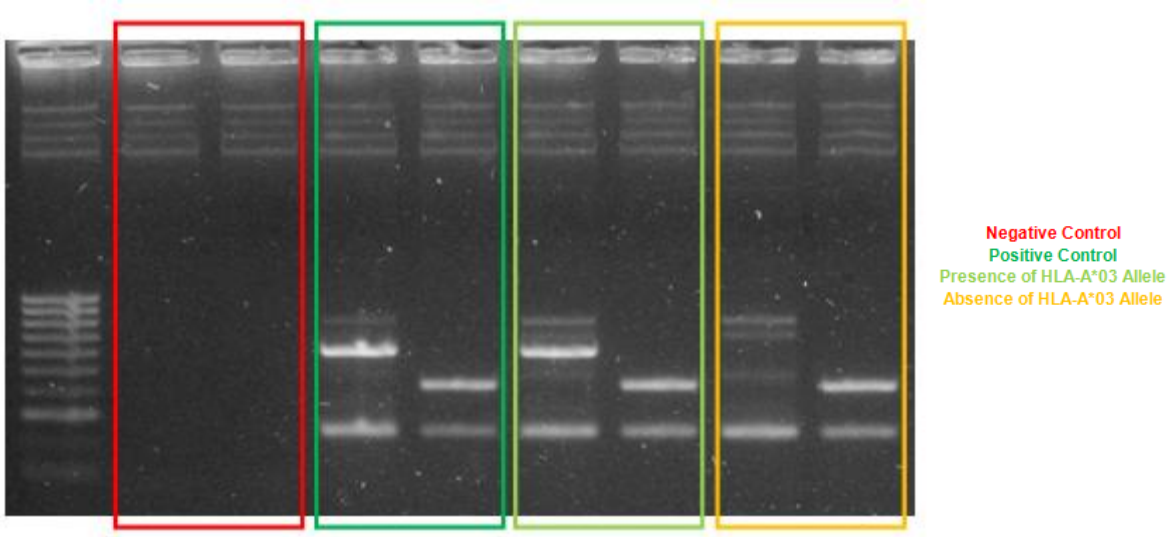

Figure 5 – HLA-A*03 allele identification through appropriate-sized bands on the gel.

The identification of the HLA-A*03 allele was performed only in 33 patients, since some patients had passed away, others remained unreachable and others simply refused to participate in this study.

6.7 Polymorphism Restriction

For the C282Y polymorphism of the HFE gene, 1 µL of RsaI enzyme (10 U/µL) was added to 1 µL of enzyme buffer. For the H63D polymorphism of the HFE gene, we added to each PCR product 0,5 µL of MboI enzyme (10 U/µL) and 2 µL of enzyme buffer.

Enzyme buffer solutions and restriction enzymes were placed and preserved on ice during the preparation of restriction mix and during distribution into the samples. Subsequently, we placed PCR tubes with the amplicons and the restriction mixes in a heated chamber, at 37ºC, overnight.

The proceedings for the production of the agarose gel were the same as previously reported, but including 9 g of agarose instead of 4,5 g (agarose gel at 3%).

The resulting solutions were placed with 2 µL of loading buffer and loaded it into the wells. In the first well of the gel, we placed a molecular weight ladder with 100 bp.

The agarose gel was visualized under a UV light and photographed. The digested products were analyzed to identify the different genotypes.

For H63D, MboI identifies and cleaves the -GATC sequence in three different sequence sites. In the absence of the polymorphism, MboI restriction creates three fragments (138, 99 and 57 bp), whereas its presence abolishes one restriction site, creating 237 and 57 bp fragments. When the three bands are visualized, the individual is considered to be homozygous-dominant (HH). Individuals are considered to be homozygous-recessive (DD), when MboI restriction creates two fragments (237 and 57 bp), because the polymorphism eliminates one site of MboI restriction. The individual is considered heterozygous (HD), if one of the alleles harbors the single nucleotide polymorphism, while the other is considered “normal”, resulting in four different fragments: 237, 137, 99 and 57 bp.

To recognize the C282Y polymorphism, we used the endonuclease RsaI, which identifies the restriction site GT’AC. This polymorphism creates a new restriction site. If the individual is homozygous dominant (CC), two fragments are observed with 203 and 140 bp length. If the individual has the polymorphism, which means he is heterozygous (CY), one additional binding site is present, thus producing four fragments (203, 111, 140 and 29 bp). If the individual harbors the single nucleotide polymorphism (SNP) in the two alleles (YY), the endonuclease cuts the fragment, producing three fragments with 203, 111 and 29 bp.

7. Statistical Analysis

In order to verify the normality of all variables, we used the Shapiro-Wilk Test. Statistical significance was calculated using Kruskal-Wallis or Mann-Whitney tests

to compare sample distribution. Person's Chi-Square was used to evaluate the differences between categorical variables and the Spearman's rank correlation coefficient to evaluate their relationship.

All analyses were undertaken using SPSS version 20 software (SPSS, Chicago, Illinois, USA). Statistical significance was accepted at $p<0,05$.

CHAPTER IV

RESULTS

1. Lesion Frequencies

Apart from the normal liver and lymph node tissues inserted as controls, TMA blocks contained 452 spots from breast samples, of which 159 disappeared during alignment, sectioning or were lost during practical procedures.

For statistical purposes, same lesions from the same case were grouped and the mean value of each parameter analyzed was taken into account. In total, 134 samples from TMA blocks were analyzed, including: 25 reduction breast reduction aesthetic surgery samples (accounted as control normal samples), 13 histologically "normal" lesions from DCIS samples, 27 pure DCIS samples, 24 histologically "normal" lesions from IDC samples, 11 DCIS lesions from IDC samples and 34 pure IDC samples.

Tissue sample and core frequencies were summarized in Table 3.

Table 3 – Tissue sample and core frequencies.

Tissue Sample	Type of Core	No. of Samples in TMA Blocks
Control Normal Samples (n=25)	**Normal**	**25**
DCIS (n=27)	Histologically "Normal" Lesions in DCIS	13
	Pure DCIS	**27**
IDC (n=34)	Histologically "Normal" Lesions in IDC	24
	DCIS in IDC	11
	Pure IDC	**34**
TOTAL		134

Abbreviations: No., Number; DCIS, Ductal Carcinoma *in situ*; IDC, Invasive Ductal Carcinoma.

2. Lymphocyte Frequencies

The immunolocalization of $CD4^+$, $CD8^+$ and $CD4^+FoxP3^+$ T-cells was observed in breast tissue samples of control normal, DCIS and IDC samples. Distinct staining patterns were apparent among samples type, as seen in the representative images illustrated in Figure 6. In general, $CD4^+$ T-lymphocytes presented a cytoplasmic

expression, $CD8^+$ T-lymphocytes a membranar expression and $FoxP3^+$ T-cells a nuclear expression.

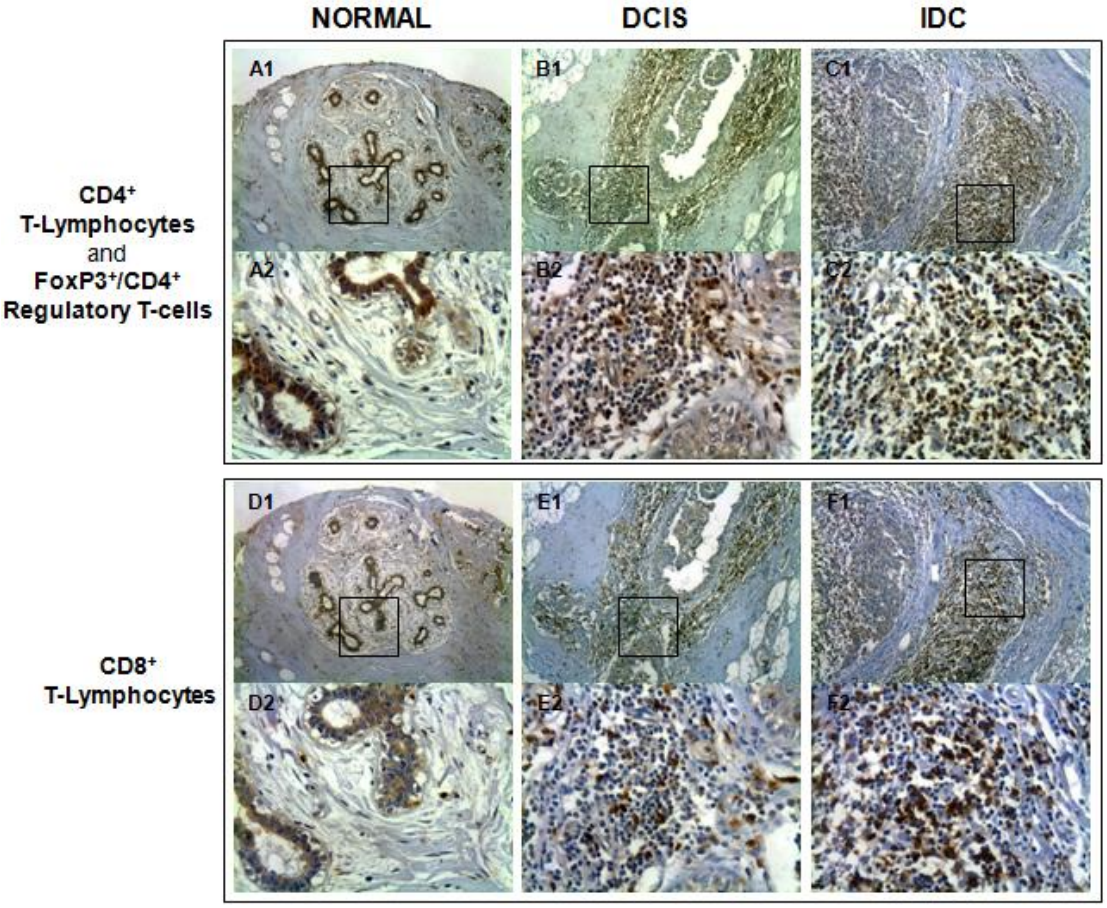

Figure 6 – Representative images of $CD4^+$ and $CD8^+$ T-lymphocytes and $CD4^+FoxP3^+$ Regulatory T-cells immunostaining in normal breast, ductal carcinoma *in situ* (DCIS) and invasive ductal carcinoma (IDC) samples. Images A1, B1, C1, D1, E1 and F1: magnification 100x; images A2, B2, C2, D2, E2 and F2: magnification 400x.

The total number of lymphocytes analyzed in this study (assessed by positivity to CD8, CD4 and FoxP3 markers) was much more pronounced in carcinoma (DCIS and IDC) than in control normal samples ($p<0,001$, $p=0,002$ and $p=0,049$, respectively).

For the purpose of this analysis, the proportion between $CD4^+$ and $CD8^+$ T-cells was evaluated by the CD4/CD8 ratio. The CD4/CD8 ratio presented a tendency to decrease from normal to IDC samples, but the differences were not statistically significant ($p=0,348$).

These results are illustrated in Figures 7, 8 and 9 (cf. Supplementary Material, Table 11).

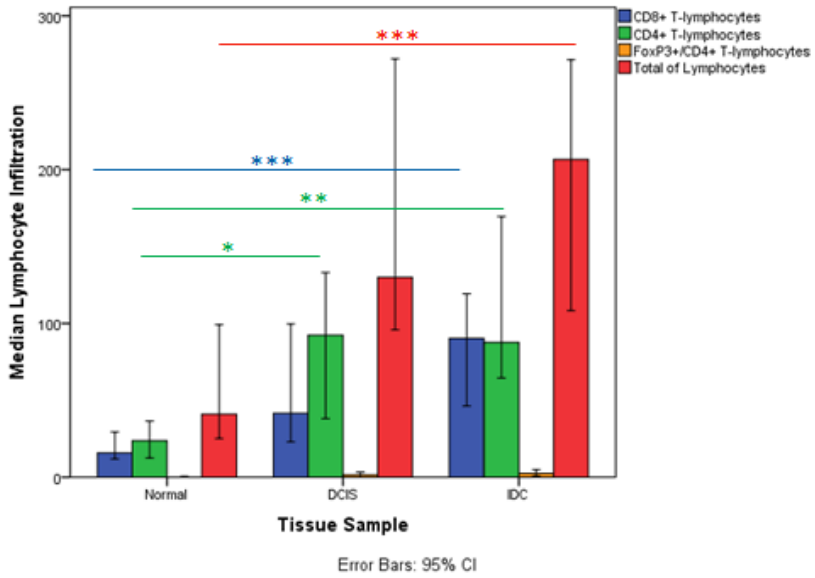

Figure 7 – Lymphocyte frequencies in breast tissue samples. Median infiltration of $CD8^+$ T-lymphocytes, $CD4^+$ T-lymphocytes, $CD4^+FoxP3^+$ T-lymphocytes and the median number of total lymphocytes in control normal (n=25, n=17, n=17 and n=17, respectively), DCIS (ductal carcinoma *in situ*) (n=26, n=25, n=25 and n=24, respectively) and in IDC (invasive ductal carcinoma) (n=34, n=30, n=30 and n=30, respectively) samples. Graph shows Median and 95% Confidence Intervals (CI). Significant differences are shown for comparison with the precedent group *p< 0,05, **p< 0,01, ***p< 0,001, Mann-Whitney test.

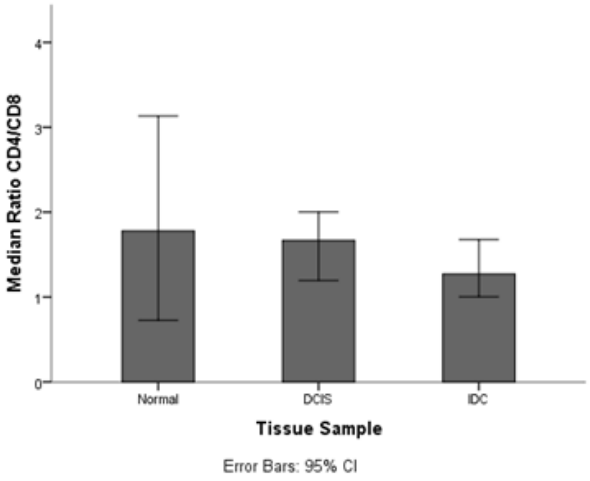

Figure 8 – CD4/CD8 ratio in breast tissue samples. Median CD4/CD8 ratio in control normal (n=16), DCIS (ductal carcinoma *in situ*) (n=24) and in IDC (invasive ductal carcinoma) (n=30) samples. Graph shows Median and 95% Confidence Intervals (CI).

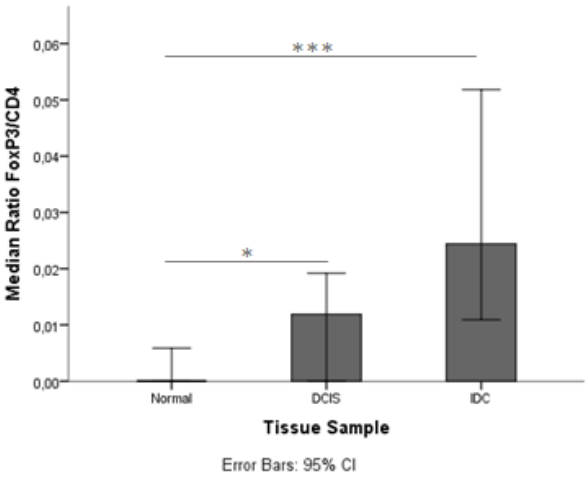

Figure 9 – FoxP3/CD4 ratio in breast tissue samples. Median FoxP3/CD4 ratio in control normal (n=17), DCIS (ductal carcinoma *in situ*) (n=25) and in IDC (invasive ductal carcinoma) (n=30) samples. Graph shows Median and 95% Confidence Intervals (CI). Significant differences are shown for comparison with the precedent group *p< 0,05, **p< 0,01, ***p< 0,001, Mann-Whitney test.

3. Ferritin Expression in Breast Tissue

Ferritin expression was mainly observed in the cytoplasm of epithelial cells and lymphocytes (Figure 10).

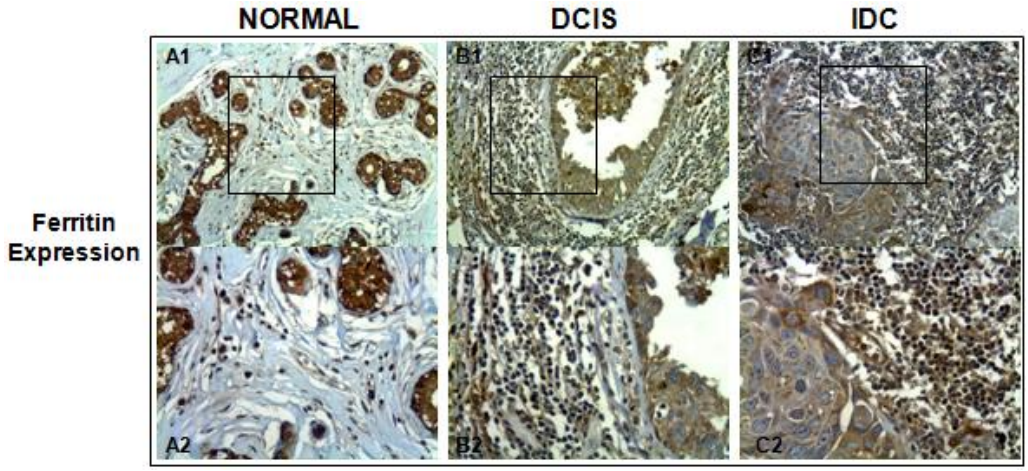

Figure 10 – Representative images of ferritin expression in normal, ductal carcinoma *in situ* (DCIS) and invasive ductal carcinoma (IDC) samples. Images A1, B1 and C1: magnification 200x; images A2, B2 and C2: magnification 400x.

Considering that the ferritin expression in epithelial cells and lymphocytes do not follow a normal distribution, non-parametric tests were performed and the median value of expression and interquartile range (IQ) were presented.

The median ferritin expression in epithelial cells in control normal samples was 15,00 (15,00-15,01), 10,00 (8,00-12,50) in DCIS samples and 10,00 (10,00-10,83) in IDC samples.

Breast cancer epithelial cells from DCIS and IDC samples presented a significantly lower median expression of ferritin than normal samples (p<0,001)

(Figure 11). There were no statistically significant differences for median ferritin expression in epithelial cells between DCIS and IDC samples (p>0,05) (Figure 11).

On the other hand, median ferritin expression in breast cancer infiltrating lymphocytes was significantly higher than in normal samples (p<0,001) (Figure 11). There were no statistically significant differences for median ferritin expression in lymphocytes between DCIS and IDC samples (p>0,05) (Figure 11).

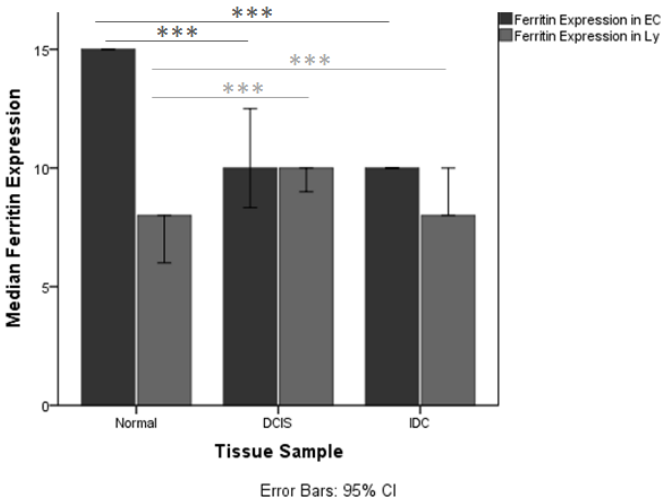

Figure 11 – Median ferritin expression in epithelial cells (EC) and lymphocytes (Ly) from control normal (n=25 and n=15, respectively), DCIS (ductal carcinoma *in situ*) (n=22 and n=17, respectively) and IDC (invasive ductal carcinoma) (n=33 and n=32, respectively) samples. Graph shows Median and 95% Confidence Intervals (CI). Significant differences are shown for comparison with the precedent group *p< 0,05, **p< 0,01, ***p< 0,001, Mann-Whitney test.

4. Nuclear Ferritin Expression

In this project, we considered the presence of nuclear ferritin in more than 10% of the epithelial cells. So, as shown in Table 4, over half of all cases presented nuclear ferritin expression, independently of sample diagnosis.

Chi-square test was performed to verify the percentage of cases with more than 10% of epithelial cells was presenting nuclear ferritin expression in breast tissue samples. We noted that the presence of nuclear ferritin had a slight tendency to increase in DCIS samples than normal or IDC samples (p>0,05). However, as the percentage of DCIS and IDC samples presenting nuclear ferritin expression was similar, we decided to group these lesions.

Comparing normal to breast ductal carcinoma samples, we observed that the presence of nuclear ferritin was not associated with the sample diagnosis (p=0,392).

Results are illustrated in Table 4.

Table 4 – Percentage of breast tissue samples presenting nuclear ferritin in epithelial cells.

	Nuclear Ferritin Expression				
	Absence		Presence		
Tissue Sample	n	%	n	%	***p***
Normal	11	44%	14	56%	**p=0,392**
Carcinoma	18	34%	35	66%	

Abbreviations: %, Percentage.

5. Ferritin in Breast Tissue and Nuclear Ferritin Expression

Considering that the ferritin expression in breast tissue does not follow a normal distribution, non-parametric tests were performed and the median value of expression and interquartile range (IQ) were presented. Mann-Whitney non-parametric test was applied to verify if the median ferritin expression in epithelial cells and lymphocytes was significantly different between samples which presenting or not nuclear ferritin in more than 10% of its epithelial cells.

No statistically significant differences were found for median ferritin expression in epithelial cells or lymphocytes, according to the presence or absence of nuclear ferritin expression (p>0,05) (Table 5).

Table 5 – Median ferritin expression in breast tissue depending on the presence of nuclear ferritin.

	Nuclear Ferritin Expression			
	Absence		Presence	
Ferritin Expression	n	Median (IQ)	n	Median (IQ)
Epithelial Cells	29	10,0 (10,0-12,5)	49	11,7 (10,0-15,0)
p	**p=0,474**			
Lymphocytes	23	8,0 (8,0-10,0)	39	8,0 (7,3-10,0)
p	**p=0,412**			

Abbreviations: IQ, Interquartile Range.

6. Lymphocytic Profile and Ferritin Expression

The lymphocytic profile was assessed through analysis of CD4/CD8 and FoxP3/CD4 median ratios. The Spearman correlation coefficient was used to determine if the CD4/CD8 ratio and FoxP3/CD4 ratio were linearly correlated with median ferritin expression in lymphocytes.

The CD4/CD8 ratio was not correlated with the median ferritin expression in lymphocytes (n=57; p=0,663; r=0,059) (Figure 12). However, the FoxP3/CD4 ratio was positively correlated with the median ferritin expression in lymphocytes (n=57; p=0,002; r=0,408) (Figure 13).

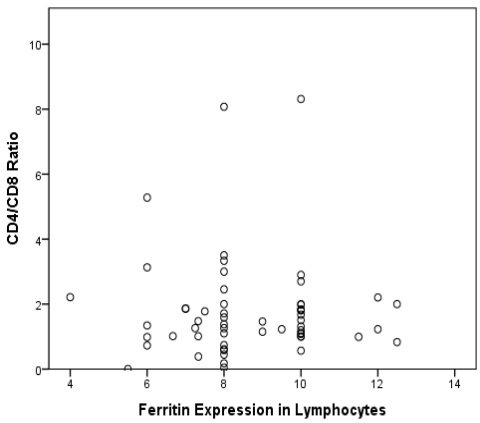

Figure 12 – Scatter diagram of Spearman's correlation coefficient between CD4/CD8 ratio and median ferritin expression in lymphocytes.

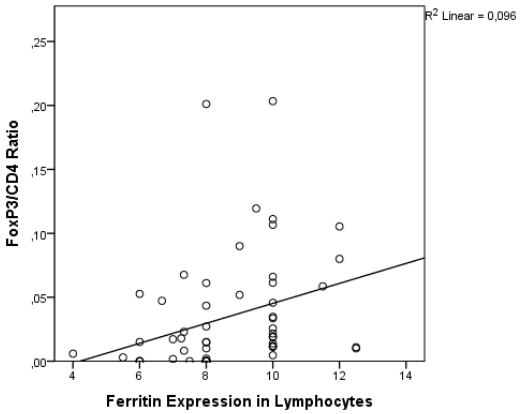

Figure 13 – Scatter diagram of Spearman's correlation coefficient between FoxP3/CD4 ratio and median ferritin expression in lymphocytes.

7. Hemosiderin Deposits, Lymphocytic Profile and Ferritin Expression

Considering that the ferritin expression and the lymphocytic profile do not follow a normal distribution, non-parametric tests were performed and the median value of expression and interquartile range (IQ) were presented. Mann-Whitney test was applied to verify if the median ferritin expression and the lymphocytic profile were associated with the presence of hemosiderin deposits in breast tissue. The lymphocytic profile was evaluated through analysis of CD4/CD8 ratio and FoxP3/CD4 ratio.

Regarding the type of lymphocytic profile, no statistically significant differences were observed, concluding that hemosiderin deposits in epithelial cells did not have effect on lymphocytic profile ($p>0,05$) (Table 6).

It was investigated if the median ferritin expression in epithelial cells and lymphocytes was associated with the presence of hemosiderin deposits in epithelial cells. No statistically significant

differences were observed regarding the accumulation of hemosiderin in epithelial cells on median ferritin expression in epithelial cells (p=0,091) and lymphocytes (p=0,611) (Table 6).

Table 6 – Lymphocytic profile and median ferritin expression according to the hemosiderin deposition in epithelial cells.

		Hemosiderin Deposits in Epithelial Cells			
		Absence		**Presence**	
		n	Median (IQ)	n	Median (IQ)
Lymphocytic Profile	Ratio CD4/CD8	41	1,34 (1,00-1,87)	28	1,63 (1,00-2,00)
	p	**p=0,608**			
	Ratio FoxP3/CD4	42	0,01 (0,00-0,05)	28	0,02 (0,00-0,05)
	p	**p=0,591**			
Ferritin Expression	Epithelial Cells	46	11,25 (10,00-15,00)	29	10,00 (7,50-12,50)
	p	**p=0,091**			
	Lymphocytes	37	8,00 (7,25-10,00)	26	8,00 (8,00-10,00)
	p	**p=0,611**			

Abbreviations: IQ, Interquartile Range.

8. Hemosiderin Deposits and Ferritin Expression

As ferritin expression in breast tissue does not follow a normal distribution, non-parametric tests were performed and the median value of expression and interquartile range (IQ) were presented. Mann-Whitney non-parametric test was applied to examine if median ferritin expression in epithelial cells and lymphocytes was associated with hemosiderin deposition in stromal inflammatory cells.

The median ferritin expression in epithelial cells was associated with hemosiderin deposition in stromal inflammatory cells (p=0,018). However, no statistically significant differences were observed for the median ferritin expression in lymphocytes, regarding the accumulation of hemosiderin in stromal inflammatory cells (p=0,958).

Results are shown in Table 7.

Table 7 – Median ferritin expression according to the hemosiderin deposition in stromal inflammatory cells.

	Hemosiderin Deposits in Stromal Inflammatory Cells			
	Absence		Presence	
Ferritin Expression	n	Median (IQ)	n	Median (IQ)
Epithelial Cells	29	10,00 (10,00-15,00)	37	10,00 (7,50-12,50)
p	**p=0,018**			
Lymphocytes	22	9,25 (7,33-10,00)	33	8,00 (8,00-10,00)
p	**p=0,958**			

Abbreviations: IQ, Interquartile Range.

9. HLA-A*03 Allele and Ferritin Expression

HLA-A*03 allele was performed in 22 of the 33 peripheral blood samples. In ductal carcinoma *in situ* (DCIS) samples, 14,3% patients presented the HLA-A*03 allele and 85,7% not. Regarding patients with invasive ductal carcinomas (IDC), the presence of HLA-A*03 allele was demonstrated in 13,3% of all cases. These results were shown in Figure 14.

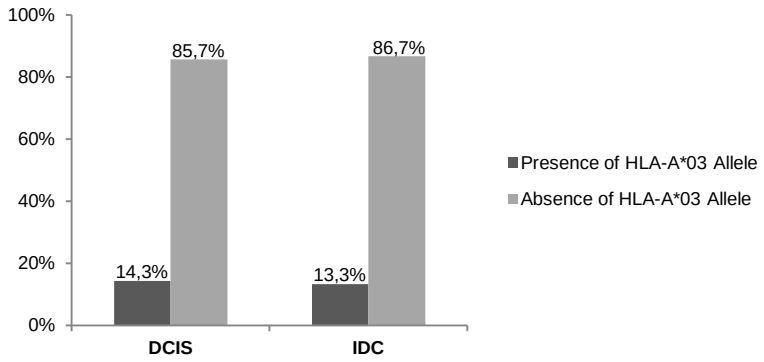

Figure 14 – Frequencies of human leukocyte antigen (HLA) HLA-A*03 allele in breast tumor samples (ductal carcinoma *in situ* (DCIS) and invasive ductal carcinoma (IDC)).

Considering that the ferritin expression does not follow a normal distribution, non-parametric tests were performed and the median value of expression and interquartile range (IQ) were presented. Mann-Whitney non-parametric test was used to determine if the median ferritin expression in epithelial cells and lymphocytes was associated with the presence or absence of the HLA-A*03 allele.

No statistically significant differences were observed regarding median ferritin expression in epithelial cells or lymphocytes, according to the presence or absence of HLA-A*03 allele (p=0,796 and p=0,071, respectively) (Table 8).

Table 8 – Median ferritin expression according to the HLA-A*03 allele.

	HLA-A*03 Allele			
	Absence		**Presence**	
Ferritin Expression	n	Median (IQ)	n	Median (IQ)
Epithelial Cells	18	10,0 (10,0-11,7)	3	10,0 (9,0-10,6)
p	**p=0,796**			
Lymphocytes	17	10,0 (8,0-10,0)	2	7,3 (6,7-8,0)
p	**p=0,071**			

Abbreviations: IQ, Interquartile Range.

In epithelial cells, independently of the absence or presence of the HLA-A*03 allele the median ferritin expression was the same (p>0,05). Nevertheless, when HLA-A*03 is present, a tendency for a lower median ferritin expression in lymphocytes was observed (p=0,071).

10. HFE Polymorphisms and Ferritin Expression

As described above, ferritin expression in epithelial cells and lymphocytes does not follow a normal distribution, hereupon, the median value of expression and interquartile range (IQ) were presented. Mann-Whitney non-parametric test was used to demonstrate if the median ferritin expression in epithelial cells and lymphocytes was associated with HFE polymorphisms.

C282Y Polymorphism

In order to reduce bias, this analysis was restricted to breast carcinoma samples, once heterozygous individuals were not identified in control samples.

No statistically significant differences were observed for median ferritin expression in epithelial cells or lymphocytes, according to the presence of the HFE C282Y polymorphism (p=0,822 and p=0,369, respectively) (Table 9).

Table 9 – Median ferritin expression according to the C282Y polymorphism.

	HFE C282Y Polymorphism			
	CC		CY	
Ferritin Expression	n	Median (IQ)	n	Median (IQ)
Epithelial Cells	44	10,00 (7,88-11,72)	8	10,00 (9,25-10,00)
p	**p=0,822**			
Lymphocytes	38	10,00 (8,00-10,00)	8	8,00 (7,63-9,88)
p	**p=0,369**			

Abbreviations: CC, Homozygous-dominant; CY, Heterozygous; IQ, Interquartile Range.

H63D Polymorphism

Even though the number of control normal population carrying the HD or DD genotype was lower than number of carcinoma samples carrying the HD or DD genotype, we verified that differences were not statistically significant for the median ferritin expression in epithelial cells and lymphocytes between normal and carcinoma samples (p>0,05) (Data not shown). We decided to use the whole population for the analysis.

No statistically significant differences were found for the median ferritin expression in epithelial cells or lymphocytes, according to the HFE H63D polymorphism (p=0,550 and p=0,885, respectively) (Table 10).

Table 10 – Median ferritin expression according to the H63D polymorphism.

	HFE H63D Polymorphism			
	HH		DD + HD	
Ferritin Expression	n	Median (IQ)	n	Median (IQ)
Epithelial Cells	41	10,0 (10,0-15,0)	34	10,4 (10,0-12,5)
p	**p=0,550**			
Lymphocytes	30	8,0 (7,3-10,0)	30	8,0 (7,5-10,0)
p	**p=0,885**			

Abbreviations: HH, Homozygous-dominant; DD, Homozygous-recessive; HD, Heterozygous; IQ, Interquartile Range.

11. Ferritin Expression, Lymphocyte Infiltration and Clinicopathological Variables of Breast Cancer Behaviour

Hormone Receptors and HER-2 Status

We extended the observation to estrogen and progesterone receptors (ER and PR, respectively) and to human epidermal growth factor 2 (HER-2) status in DCIS and IDC samples. These clinico-biological markers are associated with breast cancer behavior [69, 164]. All associations were calculated using the Mann-Whitney non-parametric test (cf. Supplementary Material, Table 12).

IDC ER positive cases presented significantly higher median ferritin expression (p=0,028).

In DCIS samples, the median number of total lymphocytes was significantly higher in ER and PR negative cases (p=0,003 and p=0,008, respectively).

$CD4^+$ T-lymphocyte median numbers were significantly higher in ER negative (p=0,002), PR negative (p=0,006) and HER-2 positive (p=0,042) cases in DCIS samples.

A higher median number of $CD8^+$ and $CD4^+FoxP3^+$ T-cells was observed in ER negative DCIS cases (p=0,009 and p=0,019, respectively).

All other comparisons were not statistically significant (p>0,05).

Tumor Size and Lymph Node Involvement

We next analyzed if the median number of lymphocytes and the median ferritin expression were associated with the local and metastatic tumor growth in invasive tumors.

No statistically significant associations were found for tumor size and lymph node involvement, according to the median numbers of $CD4^+$, $CD8^+$ and $CD4^+FoxP3^+$ T-cells, the median number of total lymphocytes and the median ferritin expression in epithelial cells and lymphocytes (p>0,05) (cf. Supplementary Material, Table 13).

CHAPTER V

DISCUSSION

1. Lymphocyte Population

The immune system has an important role in breast cancer progression [77]. $CD4^+$ and $CD8^+$ T-cells are considered the main types of lymphocytes in cell-mediated immunity and participate in anti-tumor immune responses [165]. Therefore, we compared numbers of $CD4^+$ and $CD8^+$ T-lymphocytes and the CD4/CD8 ratio between normal and carcinoma breast tissue samples (DCIS and IDC). The median numbers of $CD4^+$ and $CD8^+$ T-cells were significantly higher in tumor tissues, when compared with normal breast tissues ($p=0,002$ and $p<0,001$, respectively). Our observations are in concordance with the higher numbers of lymphocytes ($CD4^+$ and $CD8^+$ T-cells) in breast tumor samples reported in different studies [77, 166-168]. Relatively to CD4/CD8 ratio, we did not find any significant differences between normal and breast cancer samples ($p=0,348$). This finding in breast tissue is in line with a study of Schroder and colleagues [169], who did not report any significant differences in systemic CD4/CD8 ratio between controls and breast cancer samples.

Regarding regulatory T-cell numbers, assessed by the co-expression of $CD4^+$ and $FoxP3^+$ in lymphocytes, we verified an increment from normal to breast cancer samples ($p=0,049$), in agreement with other studies [94, 170-172]. Additionally, we observed that the FoxP3/CD4 ratio increases with malignancy ($p=0,018$). These results suggest the existence of a close relationship between the number of regulatory T-cells and development of cancer, suggesting that Tregs could be an important strategy for tumor escaping from anti-tumor immunity during tumor development. This is in agreement with Wang and colleagues' research, who observed that higher numbers of Tregs are associated with a poor prognosis [173].

Therefore, with our results, we can hypothesize that tumor cells are able to enhance tumor-infiltrating lymphocyte numbers, by activating anti-tumoral immune cells ($CD8^+$ cytotoxic T-cells and $CD4^+$ T-helper) or recruiting and reactivating immunosuppressive subtypes capable of tumor growth promotion, such as regulatory T-cells. Nevertheless, we cannot disregard the fact that Tregs detection was achieved through co-expression of $CD4^+$ and $FoxP3^+$ markers, not evaluating the $CD25^+$ expression [92, 173, 174], which could be argued as not reflecting activated Tregs detection.

2. Ferritin Expression

In our study, we evaluated median ferritin expression in epithelial cells in normal, DCIS and IDC samples. Breast ductal carcinoma epithelial cells presented a lower median ferritin expression ($p<0,001$) than normal samples, which confirms a previous study that they exhibit an "iron-deficiency phenotype", illustrated by the downregulation of ferritin [120]. We may consider that the control of iron homeostasis, at post-transcriptional level, is achieved through the key iron sensors, namely, iron regulatory proteins (IRPs) [3, 12]. As described above, IRPs binds to the iron-responsive elements (IREs), such as ferritin, and this ligation is regulated by intracellular iron levels, allowing cells to promptly regulate concentrations of accessible cytosolic iron [8, 27]. So, as breast cancer epithelial cells presented an "iron-utilization phenotype", IRPs are, in fact, able to interact with their target IREs which leads to the blockade of its translation and the decrease of ferritin expression [29]. Consequently, iron availability can be enhanced, dealing to an increase of hemosiderin deposits in epithelial cells. In fact, we demonstrated that a higher percentage of breast ductal carcinoma samples showed hemosiderin deposition, compared to normal controls ($p=0,022$). Munro and colleagues previously described that hemosiderin consists in a degradation product of ferritin [155]; hereupon, we hypothesized that when ferritin was downregulated, hemosiderin deposition could be enhanced. Richter and colleagues' study indicated that in individuals with hereditary hemochromatosis much of the inorganic storage iron was derived from degraded ferritin [175]. In fact, this supports our hypothesis that the majority of iron necessary for cancer cells' survival can be derived from the degradation product of ferritin.

It is well established that ferritin is a cytoplasmic iron storage protein [176]; however, several studies have reported the translocation of ferritin to the nucleus, specifically H-ferritin, which protects DNA from iron-mediated toxicity, enhancing cancer cells survival [34, 35, 122]. In view of this, we hypothesized that a higher nuclear ferritin expression could be observed in IDC samples, promoting the survival of malignant epithelial cells. Nevertheless, this hypothesis was not confirmed, once the presence of nuclear ferritin expression was not associated with sample diagnosis ($p>0,05$). We also reported no statistically significant differences for median ferritin expression in epithelial cells or lymphocytes, in line with the presence or absence of nuclear ferritin expression ($p>0,05$).

At the systemic level, the lymphocyte population represents an essential iron storage compartment, which is involved in non-transferrin-bound iron uptake [177, 178] and in a tumor supported growth, through the iron nutrition [179]. In fact, regarding hemosiderin deposits in stromal inflammatory cells, we observed an increase from normal to breast ductal carcinoma samples ($p<0,001$), bringing evidence to our hypothesis that

lymphocytes may act as an iron reservoir that assists tumor nutrition. Lymphocytes are also capable of synthesizing ferritin [44]. Alkhateeb and colleagues [120] showed, with cell lines, that extracellular ferritin stimulates breast cancer progression, independently of its iron content. In line with this information, our study revealed that, in fact, infiltrating lymphocytes display an “iron-donor” phenotype with increased median expression of ferritin in breast ductal carcinoma samples, compared with control normal samples ($p<0,001$).

We decided to identify which T-lymphocyte population(s) was/were expressing ferritin. There are consistent data concerning the association between CD4/CD8 ratio and iron stores. An example is a study performed by Porto and colleagues with hereditary hemochromatosis patients, showing that individuals with high CD4/CD8 ratios had significantly higher iron stores, compared to those with normal ratios [52]. Their study also revealed differences between individuals who were expressing the HLA-A*03 allele and those who did not expressing this allele [52]. Surprisingly, in our study, the CD4/CD8 ratio was not correlated with median ferritin expression in lymphocytes ($p=0,663$). The differences found in the present study can be explained by the reduced number of samples or the indirect method we have used to verify which T-lymphocyte population(s) was/were secreting ferritin. An alternative method for this could be the confocal immunofluorescence technique [80]. Furthermore, we cannot ignore the fact that the evaluation of ferritin expression was achieved with a polyclonal antibody, which did not discriminate the heavy and light subunits and may not considered reflect iron accumulation in these cells.

We verified that FoxP3/CD4 ratio was positively correlated with median ferritin expression in lymphocytes ($p=0,002$), which is in agreement with a study done in patients with melanoma, performed by Gray and colleagues [180]. In the same study, Gray and colleagues evidenced the importance of H-ferritin in the induction of regulatory T-cells and provided an additional insight into the suppression of immune responses in certain individuals [180].

3. HFE Gene

Advances in iron metabolism field have led to the identification of genes involved in increased cellular iron levels, such as the HFE gene [46]. Even though clinical evidence exists to support a relationship between breast cancer and HFE polymorphisms, the nature of this relationship and the mechanisms by which HFE function alters tumor progression are still unclear [181]. HFE polymorphisms have the capacity to modulate iron homeostasis by triggering serum iron overload [137]. It is already described that alterations in iron homeostasis affects tumor progression [1, 12, 38]. Neoplastic tissue

needs high levels of iron and has increased ferritin expression when compared with normal tissues [5, 12]. Individuals with hereditary hemochromatosis (C282Y homozygosity representing over 80% of HH patients found in European-derived populations [46, 182]) also present increased serum iron and ferritin concentrations, compared to those with the wild-type HFE genotype [130]. Furthermore, an earlier study, in hereditary hemochromatosis, indicated that cells from individuals expressing the HLA-A*03 antigen had a reduced ferritin secretion *in vitro,* compared to others without A3 [45]. Thus, we approached the question if HFE polymorphisms were associated with median ferritin expression in epithelial breast cancer cells and lymphocytes. Our results showed that presence of HFE, C282Y and H63D, polymorphisms are not associated with the median ferritin expression in epithelial cells and lymphocytes. These results can reflect the fact that the majority of the individuals in our cohort did not present were HFE wild-type. However, the discrepancy found with previous reports also might be due to our limited number of samples, or to the fact that our samples were histologically homogeneous (they were all from breast ductal carcinomas).

In addition to its role on iron regulation, HFE is also involved in immune system modulation [51]. In a recent work, Reuben and colleagues proposed that HFE played, in fact, a role in antigen processing and presentation leading to an inhibition of $CD8^+$ T-lymphocyte activation [51]. In fact, previous studies by Cruz and colleagues reported that the majority of hereditary hemochromatosis patients being homozygous for the C282Y polymorphism showed low $CD8^+$ T-lymphocyte numbers [183]. A recent study suggested that this abnormality of $CD8^+$ T-cell numbers in hereditary hemochromatosis could be considered a consequence of iron overload condition or a direct effect of HFE gene on the regulation of this cell population homeostasis [184]. In the present study, performed in breast cancer samples, we sought to test the hypothesis that HFE genotype could modify $CD8^+$ T-cell numbers. Our results indicated that C282Y heterozygote individuals presented an increase in $CD8^+$ T-lymphocyte median numbers in breast tissue (Data not shown). This approach contrasts with the majority of existing work. However, most available models include C282Y homozygous, and in our cohort individuals were C282Y heterozygous. The most attractive hypothesis to explain this result is the existence of a different behavior between C282Y homozygous and heterozygous individuals in a carcinogenesis context, or the existence of certain conditions showing compensatory phenotypes, suggesting that in the presence of one allele a compensating favourable effect could be observed [185].

4. HLA-A*03 Allele

Pollack and colleagues concluded that the altered ferritin secretion was associated with the HLA-A locus, by showing that individuals with the HLA-A*03 allele had a lower ferritin secretion than those without [45]. Regarding this information, we decided to examine if HLA-A*03 allele was associated with the median ferritin expression in breast cancer epithelial cells and lymphocytes. The median ferritin expression in epithelial cells and lymphocytes was not associated with the presence of the HLA-A*03 allele (p=0,796 and p=0,071, respectively). However, when the HLA-A*03 allele was present, a tendency for a median lower ferritin expression in lymphocytes was observed (p=0,071), which is in agreement with a previous referred study [45]. This tendency does not reach significance, probably due to the small number of individuals enrolled in our study.

5. Clinicopathological Variables

In the current study, we tested if the median ferritin expression and T-lymphocyte numbers were associated with established clinicopathological markers of breast cancer progression and behaviour.

To our knowledge, few studies have described an association between iron-related proteins and clinicopathological variables of breast cancer behaviour. One of these studies was performed by Jezequel and colleagues, and showed that ferritin light chain, in stromal cells, may be considered as a prognostic marker in node-negative breast cancer patients [119]. Another recent report demonstrated, for the first time, an association between the expression of iron-related proteins and the negative hormone receptor status in DCIS and tumor size [186]. These significant associations reinforce the contribution of stromal inflammatory cells for tumor progression. Regarding our results, IDC ER positive cases presented a significantly higher median ferritin expression ($p<0,05$).

Some studies had already focused on the establishment of associations between the immune profile in the tumor and recognized clinicopathological markers of breast cancer outcome [164, 187]. In DCIS samples, our results demonstrated that the median number of total lymphocytes was significantly higher in hormone receptor negative cases ($p<0,05$). Also in DCIS samples, $CD4^+$ T-lymphocyte median numbers were significantly higher in ER negative, PR negative and HER-2 positive cases ($p<0,05$). A higher median number of $CD8^+$ and $CD4^+FoxP3^+$ T-cells was observed in ER negative DCIS cases ($p<0,05$).

CHAPTER VI

CONCLUSIONS

Recent findings suggest that iron imbalances may play a critical role in the development, behaviour and progression of breast carcinogenesis. In fact, iron metabolism is emerging as a new axis of the research in breast cancer, dealing with the identification of prognostic and possibly predictive markers for therapies targeting this one. Knowing that breast cancer development and progression are influenced by epithelial cells and its microenvironment, the main goal of this study was to comprehend if a certain T-lymphocyte immune profile was associated to a higher ferritin expression, and explore if this was associated with clinicopathological markers of breast cancer progression and behaviour.

Our group has previously showed that macrophages and lymphocytes present an “iron-donor” phenotype in breast cancer tissue. However, evidences from other studies suggest that ferritin secretion by macrophages may represent a different route of iron deliver. We also demonstrated that ferritin expression in lymphocytes was not correlated with iron deposition in stromal inflammatory cells which may suggest the existence of another role for ferritin, independent of its classical function. This study supports the idea that tumor-infiltrating lymphocytes display an “iron-donor” phenotype favoring the supply of iron to proliferating breast tumor cells. These cells may control local iron homeostasis in the tumor microenvironment, being important in the regulation of tumor iron nutrition and progression.

With these results, we hope to contribute to a better understanding of breast cancer progression and behaviour.

CHAPTER VII

REFERENCES

1. Sheftel, A.D., A.B. Mason, and P. Ponka, *The long history of iron in the Universe and in health and disease.* Biochim Biophys Acta, 2012. **1820**(3): p. 161-87.
2. Marques, O., B.M. da Silva, G. Porto, and C. Lopes, *Iron homeostasis in breast cancer.* Cancer Lett, 2014. **347**(1): p. 1-14.
3. Wang, W., Z. Deng, H. Hatcher, L.D. Miller, X. Di, L. Tesfay, et al., *IRP2 regulates breast tumor growth.* Cancer Res, 2014. **74**(2): p. 497-507.
4. Pinnix, Z.K., L.D. Miller, W. Wang, R. D'Agostino, Jr., T. Kute, M.C. Willingham, et al., *Ferroportin and iron regulation in breast cancer progression and prognosis.* Sci Transl Med, 2010. **2**(43): p. 43ra56.
5. Kalinowski, D.S. and D.R. Richardson, *The evolution of iron chelators for the treatment of iron overload disease and cancer.* Pharmacol Rev, 2005. **57**(4): p. 547-83.
6. Bohnsack, B.L. and K.K. Hirschi, *Nutrient regulation of cell cycle progression.* Annu Rev Nutr, 2004. **24**: p. 433-53.
7. Andrews, N.C., *Disorders of iron metabolism.* N Engl J Med, 1999. **341**(26): p. 1986-95.
8. Hentze, M.W., M.U. Muckenthaler, B. Galy, and C. Camaschella, *Two to tango: regulation of Mammalian iron metabolism.* Cell, 2010. **142**(1): p. 24-38.
9. McCord, J.M., *Iron, free radicals, and oxidative injury.* J Nutr, 2004. **134**(11): p. 3171S-3172S.
10. Kattamis, C. and A.C. Kattamis, *Oxidative stress disturbances in erythrocytes of beta-thalassemia.* Pediatr Hematol Oncol, 2001. **18**(2): p. 85-8.
11. Kell, D.B. and E. Pretorius, *Serum ferritin is an important inflammatory disease marker, as it is mainly a leakage product from damaged cells.* Metallomics, 2014. **6**(4): p. 748-773.
12. Richardson, D.R., D.S. Kalinowski, S. Lau, P.J. Jansson, and D.B. Lovejoy, *Cancer cell iron metabolism and the development of potent iron chelators as anti-tumour agents.* Biochim Biophys Acta, 2009. **1790**(7): p. 702-17.
13. Hower, V., P. Mendes, F.M. Torti, R. Laubenbacher, S. Akman, V. Shulaev, et al., *A general map of iron metabolism and tissue-specific subnetworks.* Mol Biosyst, 2009. **5**(5): p. 422-43.
14. Andrews, N.C., *Forging a field: the golden age of iron biology.* Blood, 2008. **112**(2): p. 219-30.
15. Zhang, S., Y. Chen, W. Guo, L. Yuan, D. Zhang, Y. Xu, et al., *Disordered hepcidin-ferroportin signaling promotes breast cancer growth.* Cell Signal, 2014. **26**(11): p. 2539-50.
16. Peslova, G., J. Petrak, K. Kuzelova, I. Hrdy, P. Halada, P.W. Kuchel, et al., *Hepcidin, the hormone of iron metabolism, is bound specifically to alpha-2-macroglobulin in blood.* Blood, 2009. **113**(24): p. 6225-36.
17. Steinbicker, A.U. and M.U. Muckenthaler, *Out of balance--systemic iron homeostasis in iron-related disorders.* Nutrients, 2013. **5**(8): p. 3034-61.
18. Ross, S.L., L. Tran, A. Winters, K.J. Lee, C. Plewa, I. Foltz, et al., *Molecular mechanism of hepcidin-mediated ferroportin internalization requires ferroportin lysines, not tyrosines or JAK-STAT.* Cell Metab, 2012. **15**(6): p. 905-17.
19. Qiao, B., P. Sugianto, E. Fung, A. Del-Castillo-Rueda, M.J. Moran-Jimenez, T. Ganz, et al., *Hepcidin-induced endocytosis of ferroportin is dependent on ferroportin ubiquitination.* Cell Metab, 2012. **15**(6): p. 918-24.
20. Ganz, T. and E. Nemeth, *Hepcidin and iron homeostasis.* Biochim Biophys Acta, 2012. **1823**(9): p. 1434-43.
21. Morgan, E.H., *Transferrin, Biochemistry, Physiology and Clinical-Significance.* Molecular Aspects of Medicine, 1981. **4**(1): p. 1-123.

22. Richardson, D.R., *Potential of iron chelators as effective antiproliferative agents.* Can J Physiol Pharmacol, 1997. **75**(10-11): p. 1164-80.
23. Sipe, D.M. and R.F. Murphy, *Binding to cellular receptors results in increased iron release from transferrin at mildly acidic pH.* J Biol Chem, 1991. **266**(13): p. 8002-7.
24. Bali, P.K., O. Zak, and P. Aisen, *A new role for the transferrin receptor in the release of iron from transferrin.* Biochemistry, 1991. **30**(2): p. 324-8.
25. Cabantchik, Z.I., *Labile iron in cells and body fluids: physiology, pathology, and pharmacology.* Front Pharmacol, 2014. **5**: p. 45.
26. Buss, J.L., E. Arduini, K.C. Shephard, and P. Ponka, *Lipophilicity of analogs of pyridoxal isonicotinoyl hydrazone (PIH) determines the efflux of iron complexes and toxicity in K562 cells.* Biochem Pharmacol, 2003. **65**(3): p. 349-60.
27. Hentze, M.W., M.U. Muckenthaler, and N.C. Andrews, *Balancing acts: molecular control of mammalian iron metabolism.* Cell, 2004. **117**(3): p. 285-97.
28. Rouault, T.A., *The role of iron regulatory proteins in mammalian iron homeostasis and disease.* Nat Chem Biol, 2006. **2**(8): p. 406-14.
29. Muckenthaler, M., N.K. Gray, and M.W. Hentze, *IRP-1 binding to ferritin mRNA prevents the recruitment of the small ribosomal subunit by the cap-binding complex eIF4F.* Mol Cell, 1998. **2**(3): p. 383-8.
30. Hentze, M.W. and L.C. Kuhn, *Molecular control of vertebrate iron metabolism: mRNA-based regulatory circuits operated by iron, nitric oxide, and oxidative stress.* Proc Natl Acad Sci U S A, 1996. **93**(16): p. 8175-82.
31. Eisenstein, R.S., *Iron regulatory proteins and the molecular control of mammalian iron metabolism.* Annu Rev Nutr, 2000. **20**: p. 627-62.
32. Harrison, P.M. and P. Arosio, *The ferritins: molecular properties, iron storage function and cellular regulation.* Biochim Biophys Acta, 1996. **1275**(3): p. 161-203.
33. Recalcati, S., P. Invernizzi, P. Arosio, and G. Cairo, *New functions for an iron storage protein: the role of ferritin in immunity and autoimmunity.* J Autoimmun, 2008. **30**(1-2): p. 84-9.
34. Arosio, P., R. Ingrassia, and P. Cavadini, *Ferritins: a family of molecules for iron storage, antioxidation and more.* Biochim Biophys Acta, 2009. **1790**(7): p. 589-99.
35. Liu, N.Q., T. De Marchi, A.M. Timmermans, R. Beekhof, A.M. Trapman-Jansen, R. Foekens, et al., *Ferritin Heavy Chain in Triple Negative Breast Cancer: A Favorable Prognostic Marker that Relates to a Cluster of Differentiation 8 Positive (CD8+) Effector T-cell Response.* Mol Cell Proteomics, 2014. **13**(7): p. 1814-27.
36. Wang, J. and K. Pantopoulos, *Regulation of cellular iron metabolism.* Biochem J, 2011. **434**(3): p. 365-81.
37. Alkhateeb, A.A. and J.R. Connor, *The significance of ferritin in cancer: anti-oxidation, inflammation and tumorigenesis.* Biochim Biophys Acta, 2013. **1836**(2): p. 245-54.
38. Lamy, P.J., A. Durigova, and W. Jacot, *Iron homeostasis and anemia markers in early breast cancer.* Clin Chim Acta, 2014. **434**: p. 34-40.
39. Arosio, P., M. Yokota, and J.W. Drysdale, *Characterization of serum ferritin in iron overload: possible identity to natural apoferritin.* Br J Haematol, 1977. **36**(2): p. 199-207.
40. Jacobs, A., F. Miller, M. Worwood, M.R. Beamish, and C.A. Wardrop, *Ferritin in the serum of normal subjects and patients with iron deficiency and iron overload.* Br Med J, 1972. **4**(5834): p. 206-8.
41. Allen, K.J., L.C. Gurrin, C.C. Constantine, N.J. Osborne, M.B. Delatycki, A.J. Nicoll, et al., *Iron-overload-related disease in HFE hereditary hemochromatosis.* N Engl J Med, 2008. **358**(3): p. 221-30.
42. Guner, G., G. Kirkali, C. Yenisey, and I.R. Tore, *Cytosol and serum ferritin in breast carcinoma.* Cancer Lett, 1992. **67**(2-3): p. 103-12.
43. Bissell, M.J. and W.C. Hines, *Why don't we get more cancer? A proposed role of the microenvironment in restraining cancer progression.* Nat Med, 2011. **17**(3): p. 320-9.

44. Dorner, M.H., A. Silverstone, K. Nishiya, A. de Sostoa, G. Munn, and M. de Sousa, *Ferritin synthesis by human T lymphocytes.* Science, 1980. **209**(4460): p. 1019-21.
45. Pollack, M.S., B.M. da Silva, R.D. Moshief, S. Groshen, J. Bognacki, B. Dupont, et al., *Ferritin secretion by human mononuclear cells: association with HLA phenotype.* Clin Immunol Immunopathol, 1983. **27**(1): p. 124-34.
46. Feder, J.N., A. Gnirke, W. Thomas, Z. Tsuchihashi, D.A. Ruddy, A. Basava, et al., *A novel MHC class I-like gene is mutated in patients with hereditary haemochromatosis.* Nature Genetics, 1996. **13**(4): p. 399-408.
47. Santos, G.C., M. Zielenska, M. Prasad, and J.A. Squire, *Chromosome 6p amplification and cancer progression.* J Clin Pathol, 2007. **60**(1): p. 1-7.
48. Lebron, J.A., M.J. Bennett, D.E. Vaughn, A.J. Chirino, P.M. Snow, G.A. Mintier, et al., *Crystal structure of the hemochromatosis protein HFE and characterization of its interaction with transferrin receptor.* Cell, 1998. **93**(1): p. 111-23.
49. Feder, J.N., D.M. Penny, A. Irrinki, V.K. Lee, J.A. Lebron, N. Watson, et al., *The hemochromatosis gene product complexes with the transferrin receptor and lowers its affinity for ligand binding.* Proc Natl Acad Sci U S A, 1998. **95**(4): p. 1472-7.
50. Reuben, A., J. Godin-Ethier, M.M. Santos, and R. Lapointe, *T lymphocyte-derived TNF and IFN-gamma repress HFE expression in cancer cells.* Mol Immunol, 2015. **65**(2): p. 259-66.
51. Reuben, A., M. Phenix, M.M. Santos, and R. Lapointe, *The WT hemochromatosis protein HFE inhibits CD8(+) T-lymphocyte activation.* Eur J Immunol, 2014. **44**(6): p. 1604-14.
52. Porto, G., C. Vicente, M.A. Teixeira, O. Martins, J.M. Cabeda, R. Lacerda, et al., *Relative impact of HLA phenotype and CD4-CD8 ratios on the clinical expression of hemochromatosis.* Hepatology, 1997. **25**(2): p. 397-402.
53. Porto, G. and M. De Sousa, *Iron overload and immunity.* World J Gastroenterol, 2007. **13**(35): p. 4707-15.
54. Pietrangelo, A., *Medical progress - Hereditary hemochromatosis - A new look at an old disease.* New England Journal of Medicine, 2004. **350**(23): p. 2383-2397.
55. Silva, M.B.d.J.D., *Importância do Complexo Major de Histocompatibilidade na Prática e na Investigação Clínica.* 1989: p. 326. Dissertação (Doutorado em Ciências Biomédicas) – Instituto de Ciências Biomédicas de Abel Salazar. Universidade do Porto, Porto.
56. Waheed, A., S. Parkkila, X.Y. Zhou, S. Tomatsu, Z. Tsuchihashi, J.N. Feder, et al., *Hereditary hemochromatosis: effects of C282Y and H63D mutations on association with beta2-microglobulin, intracellular processing, and cell surface expression of the HFE protein in COS-7 cells.* Proc Natl Acad Sci U S A, 1997. **94**(23): p. 12384-9.
57. Ferlay J, S.I., Ervik M, Dikshit R, Eser S, Mathers C, Rebelo M, Parkin DM, Forman D, Bray, F. GLOBOCAN 2012 v1.0, *Cancer Incidence and Mortality Worldwide: IARC CancerBase No. 11 [Internet].* Lyon, France: International Agency for Research on Cancer. Available from: http://globocan.iarc.fr, accessed on 30/June/2015., 2013.
58. Vinay Kumar, A.A., Jon Aster, *The Breast*, in *Robins and Cotran Pathologic Basic of Disease*. 2010, Elsevier.
59. Richie, R.C. and J.O. Swanson, *Breast cancer: a review of the literature.* J Insur Med, 2003. **35**(2): p. 85-101.
60. Ginsburg, O.M. and R.R. Love, *Breast cancer: a neglected disease for the majority of affected women worldwide.* Breast J, 2011. **17**(3): p. 289-95.
61. DeVita, *Cancer of the Breast*, in *DeVita, Hellman & Rosenberg's Cancer: Principles & Practice of Oncology*, L.W. Wilkins, Editor. 2008.
62. Ritchie, M.D., L.W. Hahn, N. Roodi, L.R. Bailey, W.D. Dupont, F.F. Parl, et al., *Multifactor-dimensionality reduction reveals high-order interactions among estrogen-metabolism genes in sporadic breast cancer.* Am J Hum Genet, 2001. **69**(1): p. 138-47.
63. Ellisen, L.W. and D.A. Haber, *Hereditary breast cancer.* Annu Rev Med, 1998. **49**: p. 425-36.

64. McPherson, K., C.M. Steel, and J.M. Dixon, *ABC of breast diseases. Breast cancer-epidemiology, risk factors, and genetics.* BMJ, 2000. **321**(7261): p. 624-8.
65. Siegel, R., C. DeSantis, K. Virgo, K. Stein, A. Mariotto, T. Smith, et al., *Cancer treatment and survivorship statistics, 2012.* CA Cancer J Clin, 2012. **62**(4): p. 220-41.
66. Terry, P.D. and T.E. Rohan, *Cigarette smoking and the risk of breast cancer in women: a review of the literature.* Cancer Epidemiol Biomarkers Prev, 2002. **11**(10 Pt 1): p. 953-71.
67. Singletary, K.W. and S.M. Gapstur, *Alcohol and breast cancer: review of epidemiologic and experimental evidence and potential mechanisms.* JAMA, 2001. **286**(17): p. 2143-51.
68. Seitz, H.K., C. Pelucchi, V. Bagnardi, and C. La Vecchia, *Epidemiology and pathophysiology of alcohol and breast cancer: Update 2012.* Alcohol Alcohol, 2012. **47**(3): p. 204-12.
69. Liu, S.Z., J. Lachapelle, S. Leung, D.X. Gao, W.D. Foulkes, and T.O. Nielsen, *CD8(+) lymphocyte infiltration is an independent favorable prognostic indicator in basal-like breast cancer.* Breast Cancer Research, 2012. **14**(2).
70. Ali, H.R., E. Provenzano, S.J. Dawson, F.M. Blows, B. Liu, M. Shah, et al., *Association between CD8+ T-cell infiltration and breast cancer survival in 12,439 patients.* Ann Oncol, 2014. **25**(8): p. 1536-43.
71. Seo, A.N., H.J. Lee, E.J. Kim, H.J. Kim, M.H. Jang, H.E. Lee, et al., *Tumour-infiltrating CD8+ lymphocytes as an independent predictive factor for pathological complete response to primary systemic therapy in breast cancer.* Br J Cancer, 2013. **109**(10): p. 2705-13.
72. Coussens, L.M. and Z. Werb, *Inflammation and cancer.* Nature, 2002. **420**(6917): p. 860-7.
73. Coussens, L.M. and Z. Werb, *Inflammatory cells and cancer: think different!* J Exp Med, 2001. **193**(6): p. F23-6.
74. Shankaran, V., H. Ikeda, A.T. Bruce, J.M. White, P.E. Swanson, L.J. Old, et al., *IFNgamma and lymphocytes prevent primary tumour development and shape tumour immunogenicity.* Nature, 2001. **410**(6832): p. 1107-11.
75. Dunn, G.P., L.J. Old, and R.D. Schreiber, *The immunobiology of cancer immunosurveillance and immunoediting.* Immunity, 2004. **21**(2): p. 137-48.
76. Toyokuni, S., *Role of iron in carcinogenesis: cancer as a ferrotoxic disease.* Cancer Sci, 2009. **100**(1): p. 9-16.
77. DeNardo, D.G., D.J. Brennan, E. Rexhepaj, B. Ruffell, S.L. Shiao, S.F. Madden, et al., *Leukocyte complexity predicts breast cancer survival and functionally regulates response to chemotherapy.* Cancer Discov, 2011. **1**(1): p. 54-67.
78. DeNardo, D.G., P. Andreu, and L.M. Coussens, *Interactions between lymphocytes and myeloid cells regulate pro- versus anti-tumor immunity.* Cancer Metastasis Rev, 2010. **29**(2): p. 309-16.
79. Kohrt, H.E., N. Nouri, K. Nowels, D. Johnson, S. Holmes, and P.P. Lee, *Profile of immune cells in axillary lymph nodes predicts disease-free survival in breast cancer.* PLoS Med, 2005. **2**(9): p. e284.
80. Ruffell, B., A. Au, H.S. Rugo, L.J. Esserman, E.S. Hwang, and L.M. Coussens, *Leukocyte composition of human breast cancer.* Proc Natl Acad Sci U S A, 2012. **109**(8): p. 2796-801.
81. Kim, S., A. Lee, W. Lim, S. Park, M.S. Cho, H. Koo, et al., *Zonal difference and prognostic significance of foxp3 regulatory T cell infiltration in breast cancer.* J Breast Cancer, 2014. **17**(1): p. 8-17.
82. Smyth, M.J., G.P. Dunn, and R.D. Schreiber, *Cancer immunosurveillance and immunoediting: the roles of immunity in suppressing tumor development and shaping tumor immunogenicity.* Adv Immunol, 2006. **90**: p. 1-50.
83. Lee, A.H., C.E. Gillett, K. Ryder, I.S. Fentiman, D.W. Miles, and R.R. Millis, *Different patterns of inflammation and prognosis in invasive carcinoma of the breast.* Histopathology, 2006. **48**(6): p. 692-701.
84. Rakha, E.A., M. Aleskandarany, M.E. El-Sayed, R.W. Blamey, C.W. Elston, I.O. Ellis, et al., *The prognostic significance of inflammation and medullary histological type in invasive carcinoma of the breast.* Eur J Cancer, 2009. **45**(10): p. 1780-7.

85. Inokuma, M., C. dela Rosa, C. Schmitt, P. Haaland, J. Siebert, D. Petry, et al., *Functional T cell responses to tumor antigens in breast cancer patients have a distinct phenotype and cytokine signature.* J Immunol, 2007. **179**(4): p. 2627-33.
86. Park, H., Z. Li, X.O. Yang, S.H. Chang, R. Nurieva, Y.H. Wang, et al., *A distinct lineage of CD4 T cells regulates tissue inflammation by producing interleukin 17.* Nat Immunol, 2005. **6**(11): p. 1133-41.
87. Lin, W.W. and M. Karin, *A cytokine-mediated link between innate immunity, inflammation, and cancer.* J Clin Invest, 2007. **117**(5): p. 1175-83.
88. DeNardo, D.G., J.B. Barreto, P. Andreu, L. Vasquez, D. Tawfik, N. Kolhatkar, et al., *CD4(+) T cells regulate pulmonary metastasis of mammary carcinomas by enhancing protumor properties of macrophages.* Cancer Cell, 2009. **16**(2): p. 91-102.
89. Levings, M.K., R. Sangregorio, and M.G. Roncarolo, *Human cd25(+)cd4(+) t regulatory cells suppress naive and memory T cell proliferation and can be expanded in vitro without loss of function.* J Exp Med, 2001. **193**(11): p. 1295-302.
90. Lee, S., E.Y. Cho, Y.H. Park, J.S. Ahn, and Y.H. Im, *Prognostic impact of FOXP3 expression in triple-negative breast cancer.* Acta Oncol, 2013. **52**(1): p. 73-81.
91. Elias J. Sayour, P.M., Roger McLendon, Gabriel De Leon, Renee Reynolds, Jesse Kresak, John H. Sampson, Duane A. Mitchell, *Increased proportion of Foxp3+ regulatory T cells in tumor infiltrating lymphocytes is associated with tumor recurrence and reduced survival in patients with glioblastoma.* Springer, 2014.
92. Gokmen-Polar, Y., M.A. Thorat, P. Sojitra, R. Saxena, and S. Badve, *FOXP3 expression and nodal metastasis of breast cancer.* Cell Oncol (Dordr), 2013. **36**(5): p. 405-9.
93. Takenaka, M., N. Seki, U. Toh, S. Hattori, A. Kawahara, T. Yamaguchi, et al., *FOXP3 expression in tumor cells and tumor-infiltrating lymphocytes is associated with breast cancer prognosis.* Mol Clin Oncol, 2013. **1**(4): p. 625-632.
94. Bates, G.J., S.B. Fox, C. Han, R.D. Leek, J.F. Garcia, A.L. Harris, et al., *Quantification of regulatory T cells enables the identification of high-risk breast cancer patients and those at risk of late relapse.* J Clin Oncol, 2006. **24**(34): p. 5373-80.
95. Khong, H.T. and N.P. Restifo, *Natural selection of tumor variants in the generation of "tumor escape" phenotypes.* Nat Immunol, 2002. **3**(11): p. 999-1005.
96. Roncador, G., P.J. Brown, L. Maestre, S. Hue, J.L. Martinez-Torrecuadrada, K.L. Ling, et al., *Analysis of FOXP3 protein expression in human CD4+CD25+ regulatory T cells at the single-cell level.* Eur J Immunol, 2005. **35**(6): p. 1681-91.
97. Semenza, G.L., *Hypoxia and cancer.* Cancer Metastasis Rev, 2007. **26**(2): p. 223-4.
98. Wenger, R.H., *Mammalian oxygen sensing, signalling and gene regulation.* J Exp Biol, 2000. **203**(Pt 8): p. 1253-63.
99. Toyokuni, S., *Iron-induced carcinogenesis: the role of redox regulation.* Free Radic Biol Med, 1996. **20**(4): p. 553-66.
100. Jian, J., Q. Yang, J. Dai, J. Eckard, D. Axelrod, J. Smith, et al., *Effects of iron deficiency and iron overload on angiogenesis and oxidative stress-a potential dual role for iron in breast cancer.* Free Radic Biol Med, 2011. **50**(7): p. 841-7.
101. Kwok, J.C. and D.R. Richardson, *The iron metabolism of neoplastic cells: alterations that facilitate proliferation?* Crit Rev Oncol Hematol, 2002. **42**(1): p. 65-78.
102. Brookes, M.J., S. Hughes, F.E. Turner, G. Reynolds, N. Sharma, T. Ismail, et al., *Modulation of iron transport proteins in human colorectal carcinogenesis.* Gut, 2006. **55**(10): p. 1449-60.
103. Boult, J., K. Roberts, M.J. Brookes, S. Hughes, J.P. Bury, S.S. Cross, et al., *Overexpression of cellular iron import proteins is associated with malignant progression of esophageal adenocarcinoma.* Clin Cancer Res, 2008. **14**(2): p. 379-87.
104. Torti, S.V. and F.M. Torti, *Cellular iron metabolism in prognosis and therapy of breast cancer.* Crit Rev Oncog, 2013. **18**(5): p. 435-48.

105. Larrick, J.W. and P. Cresswell, *Modulation of cell surface iron transferrin receptors by cellular density and state of activation.* J Supramol Struct, 1979. **11**(4): p. 579-86.
106. Richardson, D.R. and E. Baker, *The uptake of iron and transferrin by the human malignant melanoma cell.* Biochim Biophys Acta, 1990. **1053**(1): p. 1-12.
107. Trinder, D., O. Zak, and P. Aisen, *Transferrin receptor-independent uptake of differic transferrin by human hepatoma cells with antisense inhibition of receptor expression.* Hepatology, 1996. **23**(6): p. 1512-20.
108. Trowbridge, I.S. and F. Lopez, *Monoclonal antibody to transferrin receptor blocks transferrin binding and inhibits human tumor cell growth in vitro.* Proc Natl Acad Sci U S A, 1982. **79**(4): p. 1175-9.
109. Taetle, R., J.M. Honeysett, and I. Trowbridge, *Effects of anti-transferrin receptor antibodies on growth of normal and malignant myeloid cells.* Int J Cancer, 1983. **32**(3): p. 343-9.
110. Habashy, H.O., D.G. Powe, C.M. Staka, E.A. Rakha, G. Ball, A.R. Green, et al., *Transferrin receptor (CD71) is a marker of poor prognosis in breast cancer and can predict response to tamoxifen.* Breast Cancer Res Treat, 2010. **119**(2): p. 283-93.
111. Richardson, D.R. and P. Ponka, *The molecular mechanisms of the metabolism and transport of iron in normal and neoplastic cells.* Biochim Biophys Acta, 1997. **1331**(1): p. 1-40.
112. Rossiello, R., M.V. Carriero, and G.G. Giordano, *Distribution of ferritin, transferrin and lactoferrin in breast carcinoma tissue.* J Clin Pathol, 1984. **37**(1): p. 51-5.
113. Keown, P. and B. Descamps-Latscha, *In vitro suppression of cell-mediated immunity by ferroproteins and ferric salts.* Cell Immunol, 1983. **80**(2): p. 257-66.
114. Marcus, D.M. and N. Zinberg, *Measurement of serum ferritin by radioimmunoassay: results in normal individuals and patients with breast cancer.* J Natl Cancer Inst, 1975. **55**(4): p. 791-5.
115. Kew, M.C., J.D. Torrance, D. Derman, M. Simon, G.M. Macnab, R.W. Charlton, et al., *Serum and tumour ferritins in primary liver cancer.* Gut, 1978. **19**(4): p. 294-9.
116. Hann, H.W., H.M. Levy, and A.E. Evans, *Serum ferritin as a guide to therapy in neuroblastoma.* Cancer Res, 1980. **40**(5): p. 1411-3.
117. Weinstein, R.E., B.H. Bond, and B.K. Silberberg, *Tissue ferritin concentration in carcinoma of the breast.* Cancer, 1982. **50**(11): p. 2406-9.
118. Jacobs, A., B. Jones, C. Ricketts, R.D. Bulbrook, and D.Y. Wang, *Serum ferritin concentration in early breast cancer.* Br J Cancer, 1976. **34**(3): p. 286-90.
119. Jezequel, P., L. Campion, F. Spyratos, D. Loussouarn, M. Campone, C. Guerin-Charbonnel, et al., *Validation of tumor-associated macrophage ferritin light chain as a prognostic biomarker in node-negative breast cancer tumors: A multicentric 2004 national PHRC study.* Int J Cancer, 2012. **131**(2): p. 426-37.
120. Alkhateeb, A.A., B. Han, and J.R. Connor, *Ferritin stimulates breast cancer cells through an iron-independent mechanism and is localized within tumor-associated macrophages.* Breast Cancer Res Treat, 2013. **137**(3): p. 733-44.
121. Shpyleva, S.I., V.P. Tryndyak, O. Kovalchuk, A. Starlard-Davenport, V.F. Chekhun, F.A. Beland, et al., *Role of ferritin alterations in human breast cancer cells.* Breast Cancer Res Treat, 2011. **126**(1): p. 63-71.
122. Wu, K.J., A. Polack, and R. Dalla-Favera, *Coordinated regulation of iron-controlling genes, H-ferritin and IRP2, by c-MYC.* Science, 1999. **283**(5402): p. 676-9.
123. Summers, M.R. and A. Jacobs, *Iron uptake and ferritin synthesis by peripheral blood leucocytes from normal subjects and patients with iron deficiency and the anaemia of chronic disease.* Br J Haematol, 1976. **34**(2): p. 221-9.
124. Cohen, L.A., L. Gutierrez, A. Weiss, Y. Leichtmann-Bardoogo, D.L. Zhang, D.R. Crooks, et al., *Serum ferritin is derived primarily from macrophages through a nonclassical secretory pathway.* Blood, 2010. **116**(9): p. 1574-84.

125. Ferring-Appel, D., M.W. Hentze, and B. Galy, *Cell-autonomous and systemic context-dependent functions of iron regulatory protein 2 in mammalian iron metabolism.* Blood, 2009. **113**(3): p. 679-87.
126. Jones, B.M., M. Worwood, and A. Jacobs, *Serum ferritin in patients with cancer: determination with antibodies to HeLa cell and spleen ferritin.* Clin Chim Acta, 1980. **106**(2): p. 203-14.
127. Robertson, J.F., D. Pearson, M.R. Price, C. Selby, J. Pearson, R.W. Blamey, et al., *Prospective assessment of the role of five tumour markers in breast cancer.* Cancer Immunol Immunother, 1991. **33**(6): p. 403-10.
128. Moroz, C., N. Lahat, M. Biniaminov, and B. Ramot, *Ferritin on the surface of lymphocytes in Hodgkin's disease patients. A possible blocking substance removed by levamisole.* Clin Exp Immunol, 1977. **29**(1): p. 30-5.
129. Diep, C.B., L.A. Parada, M.R. Teixeira, M. Eknaes, J.M. Nesland, B. Johansson, et al., *Genetic profiling of colorectal cancer liver metastases by combined comparative genomic hybridization and G-banding analysis.* Genes Chromosomes Cancer, 2003. **36**(2): p. 189-97.
130. Osborne, N.J., L.C. Gurrin, K.J. Allen, C.C. Constantine, M.B. Delatycki, C.E. McLaren, et al., *HFE C282Y homozygotes are at increased risk of breast and colorectal cancer.* Hepatology, 2010. **51**(4): p. 1311-8.
131. Hsing, A.W., J.K. McLaughlin, J.H. Olsen, L. Mellemkjar, S. Wacholder, and J.F. Fraumeni, Jr., *Cancer risk following primary hemochromatosis: a population-based cohort study in Denmark.* Int J Cancer, 1995. **60**(2): p. 160-2.
132. Stevens, R.G., D.Y. Jones, M.S. Micozzi, and P.R. Taylor, *Body iron stores and the risk of cancer.* N Engl J Med, 1988. **319**(16): p. 1047-52.
133. Knekt, P., A. Reunanen, H. Takkunen, A. Aromaa, M. Heliovaara, and T. Hakulinen, *Body iron stores and risk of cancer.* Int J Cancer, 1994. **56**(3): p. 379-82.
134. Stevens, R.G., B.I. Graubard, M.S. Micozzi, K. Neriishi, and B.S. Blumberg, *Moderate elevation of body iron level and increased risk of cancer occurrence and death.* Int J Cancer, 1994. **56**(3): p. 364-9.
135. Nelson, R.L., F.G. Davis, E. Sutter, L.H. Sobin, J.W. Kikendall, and P. Bowen, *Body iron stores and risk of colonic neoplasia.* J Natl Cancer Inst, 1994. **86**(6): p. 455-60.
136. Beckman, L.E., G.F. Van Landeghem, C. Sikstrom, A. Wahlin, B. Markevarn, G. Hallmans, et al., *Interaction between haemochromatosis and transferrin receptor genes in different neoplastic disorders.* Carcinogenesis, 1999. **20**(7): p. 1231-3.
137. Liu, X., C. Lv, X. Luan, and M. Lv, *C282Y polymorphism in the HFE gene is associated with risk of breast cancer.* Tumour Biol, 2013. **34**(5): p. 2759-64.
138. Gurrin, L.C., N.A. Bertalli, G.W. Dalton, N.J. Osborne, C.C. Constantine, C.E. McLaren, et al., *HFE C282Y/H63D compound heterozygotes are at low risk of hemochromatosis-related morbidity.* Hepatology, 2009. **50**(1): p. 94-101.
139. Hunt, J.R. and H. Zeng, *Iron absorption by heterozygous carriers of the HFE C282Y mutation associated with hemochromatosis.* Am J Clin Nutr, 2004. **80**(4): p. 924-31.
140. Kondrashova, T.V., K. Neriishi, S. Ban, T.I. Ivanova, L.I. Krikunova, N.I. Shentereva, et al., *Frequency of hemochromatosis gene (HFE) mutations in Russian healthy women and patients with estrogen-dependent cancers.* Biochim Biophys Acta, 2006. **1762**(1): p. 59-65.
141. Gunel-Ozcan, A., S. Alyilmaz-Bekmez, E.N. Guler, and D. Guc, *HFE H63D mutation frequency shows an increase in Turkish women with breast cancer.* BMC Cancer, 2006. **6**: p. 37.
142. Zhang, M., H. Xiong, L. Fang, W. Lu, X. Wu, Y.Q. Wang, et al., *Meta-Analysis of the Association between H63D and C282Y Polymorphisms in HFE and Cancer Risk.* Asian Pac J Cancer Prev, 2015. **16**(11): p. 4633-9.

143. Gannon, P.O., S. Medelci, C. Le Page, M. Beaulieu, D.M. Provencher, A.M. Mes-Masson, et al., *Impact of hemochromatosis gene (HFE) mutations on epithelial ovarian cancer risk and prognosis.* Int J Cancer, 2011. **128**(10): p. 2326-34.
144. Abraham, B.K., C. Justenhoven, B. Pesch, V. Harth, G. Weirich, C. Baisch, et al., *Investigation of genetic variants of genes of the hemochromatosis pathway and their role in breast cancer.* Cancer Epidemiol Biomarkers Prev, 2005. **14**(5): p. 1102-7.
145. Batschauer, A.P., N.G. Cruz, V.C. Oliveira, F.F. Coelho, I.R. Santos, M.T. Alves, et al., *HFE, MTHFR, and FGFR4 genes polymorphisms and breast cancer in Brazilian women.* Mol Cell Biochem, 2011. **357**(1-2): p. 247-53.
146. Yaouanq, J., M. Perichon, M. Chorney, P. Pontarotti, A. Le Treut, A. el Kahloun, et al., *Anonymous marker loci within 400 kb of HLA-A generate haplotypes in linkage disequilibrium with the hemochromatosis gene (HFE).* Am J Hum Genet, 1994. **54**(2): p. 252-63.
147. Simon, M., M. Bourel, R. Fauchet, and B. Genetet, *Association of HLA-A3 and HLA-B14 antigens with idiopathic haemochromatosis.* Gut, 1976. **17**(5): p. 332-4.
148. Thomas, W., A. Fullan, D.B. Loeb, E.E. McClelland, B.R. Bacon, and R.K. Wolff, *A haplotype and linkage disequilibrium analysis of the hereditary hemochromatosis gene region.* Human Genetics, 1998. **102**(5): p. 517-525.
149. de Almeida, S.F., I.F. Carvalho, C.S. Cardoso, J.V. Cordeiro, J.E. Azevedo, J. Neefjes, et al., *HFE cross-talks with the MHC class I antigen presentation pathway.* Blood, 2005. **106**(3): p. 971-7.
150. Porto, G., R. Reimao, C. Goncalves, C. Vicente, B. Justica, and M. de Sousa, *Haemochromatosis as a window into the study of the immunological system: a novel correlation between CD8+ lymphocytes and iron overload.* Eur J Haematol, 1994. **52**(5): p. 283-90.
151. Arosa, F.A., L. Oliveira, G. Porto, B.M. da Silva, W. Kruijer, J. Veltman, et al., *Anomalies of the CD8+ T cell pool in haemochromatosis: HLA-A3-linked expansions of CD8+CD28- T cells.* Clin Exp Immunol, 1997. **107**(3): p. 548-54.
152. de Sousa, M. and G. Porto, *The immunological system in hemochromatosis.* J Hepatol, 1998. **28 Suppl 1**: p. 1-7.
153. Moch, H., T. Kononen, O.P. Kallioniemi, and G. Sauter, *Tissue microarrays: what will they bring to molecular and anatomic pathology?* Adv Anat Pathol, 2001. **8**(1): p. 14-20.
154. Voduc, D., C. Kenney, and T.O. Nielsen, *Tissue microarrays in clinical oncology.* Semin Radiat Oncol, 2008. **18**(2): p. 89-97.
155. Munro, H.N. and M.C. Linder, *Ferritin: structure, biosynthesis, and role in iron metabolism.* Physiol Rev, 1978. **58**(2): p. 317-96.
156. Roschzttardtz, H., G. Conejero, C. Curie, and S. Mari, *Identification of the endodermal vacuole as the iron storage compartment in the Arabidopsis embryo.* Plant Physiol, 2009. **151**(3): p. 1329-38.
157. Meguro, R., Y. Asano, S. Odagiri, C. Li, H. Iwatsuki, and K. Shoumura, *Nonheme-iron histochemistry for light and electron microscopy: a historical, theoretical and technical review.* Arch Histol Cytol, 2007. **70**(1): p. 1-19.
158. van Duijn, S., R.J. Nabuurs, S.G. van Duinen, and R. Natte, *Comparison of histological techniques to visualize iron in paraffin-embedded brain tissue of patients with Alzheimer's disease.* J Histochem Cytochem, 2013. **61**(11): p. 785-92.
159. Miller, S.A., D.D. Dykes, and H.F. Polesky, *A simple salting out procedure for extracting DNA from human nucleated cells.* Nucleic Acids Res, 1988. **16**(3): p. 1215.
160. Manak, M.M., *DNA probes*. G. H. Keller and M. M. Manak ed. Sample Preparation. 1993, New York: Stockton Press. 27-68.
161. Mullis, K., F. Faloona, S. Scharf, R. Saiki, G. Horn, and H. Erlich, *Specific enzymatic amplification of DNA in vitro: the polymerase chain reaction.* Cold Spring Harb Symp Quant Biol, 1986. **51 Pt 1**: p. 263-73.

162. Aaij, C. and P. Borst, *The gel electrophoresis of DNA.* Biochim Biophys Acta, 1972. **269**(2): p. 192-200.
163. Bunce, M., G.C. Fanning, and K.I. Welsh, *Comprehensive, serologically equivalent DNA typing for HLA-B by PCR using sequence-specific primers (PCR-SSP).* Tissue Antigens, 1995. **45**(2): p. 81-90.
164. Mahmoud, S.M., E.C. Paish, D.G. Powe, R.D. Macmillan, M.J. Grainge, A.H. Lee, et al., *Tumor-infiltrating CD8+ lymphocytes predict clinical outcome in breast cancer.* J Clin Oncol, 2011. **29**(15): p. 1949-55.
165. Riazi Rad, F., S. Ajdary, R. Omranipour, M.H. Alimohammadian, and M.H. Z, *Comparative analysis of CD4+ and CD8+ T cells in tumor tissues, lymph nodes and the peripheral blood from patients with breast cancer.* Iran Biomed J, 2015. **19**(1): p. 35-44.
166. Laguens G, C.S., Chambó J, Girolamo VD, *Stromal CD4+ and CD8+ T Cells in Human Breast Carcinomas. Its Correlation with Chemokine MIG/CXCL9.* Adv Breast Cancer Res, 2012. **1**(2): p. 7-11.
167. Dobrzanski, M.J., J.B. Reome, J.C. Hylind, and K.A. Rewers-Felkins, *CD8-mediated type 1 antitumor responses selectively modulate endogenous differentiated and nondifferentiated T cell localization, activation, and function in progressive breast cancer.* J Immunol, 2006. **177**(11): p. 8191-201.
168. Matkowski, R., I. Gisterek, A. Halon, A. Lacko, K. Szewczyk, U. Staszek, et al., *The prognostic role of tumor-infiltrating CD4 and CD8 T lymphocytes in breast cancer.* Anticancer Res, 2009. **29**(7): p. 2445-51.
169. Schroder, W., A. Vering, M. Stegmuller, and R. Strohmeier, *Lymphocyte subsets in patients with ovarian and breast cancer.* Eur J Gynaecol Oncol, 1997. **18**(6): p. 474-7.
170. Liu, F., R. Lang, J. Zhao, X. Zhang, G.A. Pringle, Y. Fan, et al., *CD8(+) cytotoxic T cell and FOXP3(+) regulatory T cell infiltration in relation to breast cancer survival and molecular subtypes.* Breast Cancer Res Treat, 2011. **130**(2): p. 645-55.
171. Lopes, L.F., R.L. Guembarovski, A.L. Guembarovski, M.O. Kishima, C.Z. Campos, J.M. Oda, et al., *FOXP3 transcription factor: a candidate marker for susceptibility and prognosis in triple negative breast cancer.* Biomed Res Int, 2014. **2014**: p. 341654.
172. Huang, Y., C. Ma, Q. Zhang, J. Ye, F. Wang, Y. Zhang, et al., *CD4+ and CD8+ T cells have opposing roles in breast cancer progression and outcome.* Oncotarget, 2015. **6**(19): p. 17462-78.
173. Wang, Z.K., B. Yang, H. Liu, Y. Hu, J.L. Yang, L.L. Wu, et al., *Regulatory T cells increase in breast cancer and in stage IV breast cancer.* Cancer Immunol Immunother, 2012. **61**(6): p. 911-6.
174. Lal, A., L. Chan, S. Devries, K. Chin, G.K. Scott, C.C. Benz, et al., *FOXP3-positive regulatory T lymphocytes and epithelial FOXP3 expression in synchronous normal, ductal carcinoma in situ, and invasive cancer of the breast.* Breast Cancer Res Treat, 2013. **139**(2): p. 381-90.
175. Richter, G.W., *The nature of storage iron in idiopathic hemochromatosis and in hemosiderosis. Electron optical, chemical, and serologic studies on isolated hemosiderin granules.* J Exp Med, 1960. **112**: p. 551-70.
176. Alkhateeb, A.A. and J.R. Connor, *Nuclear ferritin: A new role for ferritin in cell biology.* Biochim Biophys Acta, 2010. **1800**(8): p. 793-7.
177. Pinto, J.P., J. Arezes, V. Dias, S. Oliveira, I. Vieira, M. Costa, et al., *Physiological implications of NTBI uptake by T lymphocytes.* Front Pharmacol, 2014. **5**: p. 24.
178. Arezes, J., M. Costa, I. Vieira, V. Dias, X.L. Kong, R. Fernandes, et al., *Non-transferrin-bound iron (NTBI) uptake by T lymphocytes: evidence for the selective acquisition of oligomeric ferric citrate species.* PLoS One, 2013. **8**(11): p. e79870.
179. de Sousa, M., *An outsider's perspective--ecotaxis revisited: an integrative review of cancer environment, iron and immune system cells.* Integr Biol (Camb), 2011. **3**(4): p. 343-9.

180. Gray, C.P., P. Arosio, and P. Hersey, *Association of increased levels of heavy-chain ferritin with increased CD4+ CD25+ regulatory T-cell levels in patients with melanoma.* Clin Cancer Res, 2003. **9**(7): p. 2551-9.
181. Weston Cody, H.W., Nixon Anne, Neely Elizabeth, Webb Becky, Alkhateeb Ahmed, Connor James, *Host H67D Genotype Affects Tumor Growth in Mouse Melanoma.* Journal of Cancer Science & Therapy, 2015. **7**(7): p. 216-223.
182. Jouanolle, A.M., G. Gandon, P. Jezequel, M. Blayau, M.L. Campion, J. Yaouanq, et al., *Haemochromatosis and HLA-H.* Nat Genet, 1996. **14**(3): p. 251-2.
183. Cruz, E., J. Vieira, S. Almeida, R. Lacerda, A. Gartner, C.S. Cardoso, et al., *A study of 82 extended HLA haplotypes in HFE-C282Y homozygous hemochromatosis subjects: relationship to the genetic control of CD8+ T-lymphocyte numbers and severity of iron overload.* BMC Med Genet, 2006. **7**: p. 16.
184. Costa, M., E. Cruz, S. Oliveira, V. Benes, T. Ivacevic, M.J. Silva, et al., *Lymphocyte gene expression signatures from patients and mouse models of hereditary hemochromatosis reveal a function of HFE as a negative regulator of CD8+ T-lymphocyte activation and differentiation in vivo.* PLoS One, 2015. **10**(4): p. e0124246.
185. Fabio, G., M. Zarantonello, C. Mocellin, P. Bonara, C. Corengia, S. Fargion, et al., *Peripheral lymphocytes and intracellular cytokines in C282Y homozygous hemochromatosis patients.* J Hepatol, 2002. **37**(6): p. 753-61.
186. Marques, O., G. Porto, A. Rêma, F. Faria, B.M. Silva, J.P. Pinto, et al., *Iron (de)regulation in breast cancer: a role for stromal inflammatory cells in the tumor microenvironment*, in *Annals of Oncology (2014) 25 (suppl_1): i17-i18. 10.1093/annonc/mdu067*. 2014.
187. Liu, S., J. Lachapelle, S. Leung, D. Gao, W.D. Foulkes, and T.O. Nielsen, *CD8+ lymphocyte infiltration is an independent favorable prognostic indicator in basal-like breast cancer.* Breast Cancer Res, 2012. **14**(2): p. R48.

CHAPTER VIII

SUPPLEMENTARY MATERIAL

Table 11 – Median lymphocyte frequencies in breast tissue samples.

			Tissue Sample		
			Normal	**DCIS**	**IDC**
Type of Lymphocytic Profile	**CD8$^+$**	**n**	25	26	34
		Median (IQ)	12,67 (4,50-26,50)	41,66 (23,00-99,75)	87,82 (36,25-159,56)
		p	**p<0,001**		
	CD4$^+$	**n**	17	25	30
		Median (IQ)	23,75 (12,50-36,56)	89,00 (35,00-133,00)	87,57 (56,42-174,50)
		p	**p=0,002**		
	Ratio CD4/CD8	**n**	16	24	30
		Median (IQ)	1,78 (0,74-3,07)	1,67 (1,15-2,10)	1,27 (0,99-1,78)
		p	**p=0,348**		
	CD4$^+$FoxP3$^+$	**n**	17	25	30
		Median (IQ)	0,00 (0,00-0,50)	1,04 (0,00-3,33)	2,50 (0,57-7,50)
		p	**p=0,049**		
	Ratio FoxP3/CD4	**n**	17	25	30
		Median (IQ)	0,00 (0,00-0,01)	0,01 (0,00-0,03)	0,02 (0,01-0,06)
		p	**p=0,018**		
	Total of Ly	**n**	17	24	30
		Median (IQ)	41,05 (25,17-99,14)	129,94 (86,63-276,10)	206,68 (97,92-283,96)
		p	**p=0,001**		

Abbreviations: Ly, Lymphocytes; IQ, Interquartile Range; DCIS, Ductal Carcinoma *in situ*; IDC, Invasive Ductal Carcinoma.

Table 12 – Median ferritin expression and lymphocytic infiltration according to the hormone receptor status.

	Clinicopathological Variable	ER status		PR status		HER-2 status	
		ER^-	ER^+	PR^-	PR^+	$HER\text{-}2^-$	$HER\text{-}2^+$
DCIS	**$CD4^+$ T-ly** Median (IQ)	148,04 (113,71-211,37)	62,50 (28,83-89,00)	148,04 (101,67-211,00)	62,50 (31,92-81,97)	38,10 (23,33-97,50)	102,50 (86,13-146,07)
	n	8	13	10	11	13	9
	p	**p=0,002**		**p=0,006**		**p=0,042**	
	$CD8^+$ T-ly Median (IQ)	110,96 (65,72-138,88)	33,67 (23,00-51,32)	94,31 (33,67-144,00)	37,53 (24,42-66,91)	37,53 (20,00-122,17)	51,32 (33,67-99,75)
	n	8	13	10	11	13	9
	p	**p=0,009**		**p=0,067**		**p=0,483**	
	Ratio CD4/CD8 Median (IQ)	1,41 (1,21-1,92)	1,82 (1,24-2,55)	1,67 (1,23-2,00)	1,68 (1,02-2,21)	1,21 (0,63-1,88)	1,87 (1,49-2,70)
	n	8	12	10	10	12	9
	p	**p=0,512**		**p=0,910**		**p=0,060**	
	$CD4^+FoxP3^+$ Ly Median (IQ)	3,42 (2,53-6,85)	0,00 (0,00-1,04)	3,42 (0,00-8,00)	0,17 (0,00-1,42)	0,00 (0,00-5,00)	2,25 (0,83-3,33)
	n	8	13	10	11	13	9
	p	**p=0,019**		**p=0,055**		**p=0,452**	
	Ratio FoxP3/CD4 Median (IQ)	0,02 (0,01-0,06)	0,00 (0,00-0,01)	0,02 (0,00-0,07)	0,00 (0,00-0,02)	0,00 (0,00-0,05)	0,01 (0,01-0,02)
	n	8	13	10	11	13	9
	p	**p=0,109**		**p=0,294**		**p=0,784**	
	Total of Ly Median (IQ)	285,11 (197,21-323,59)	105,41 (67,71-127,00)	285,11 (136,17-329,50)	105,41 (77,43-117,83)	102,42 (44,94-281,08)	147,24 (123,71-280,13)
	n	8	12	10	10	12	9
	p	**p=0,003**		**p=0,008**		**p=0,118**	
	Ft Expression in EC Median (IQ)	10,00 (10,00-11,79)	10,00 (8,00-11,25)	10,00 (10,00-11,07)	10,00 (8,00-12,50)	10,00 (8,00-11,25)	10,00 (9,00-12,50)
	n	7	11	9	9	11	9
	p	**p=0,403**		**p=0,928**		**p=0,726**	
	Ft Expression in Ly Median (IQ)	10,00 (9,75-10,00)	9,00 (7,00-10,00)	10,00 (9,75-10,00)	8,13 (7,00-10,00)	9,25 (8,50-10,00)	10,00 (8,63-10,00)
	n	7	6	7	6	8	7
	p	**p=0,185**		**p=0,122**		**p=0,473**	
IDC	**$CD4^+$ T-ly** Median (IQ)	154,42 (49,36-172,89)	79,82 (58,58-178,90)	56,41 (33,53-175,28)	93,75 (69,53-156,92)	78,25 (55,05-154,07)	169,50 (97,88-208,30)
	n	6	24	11	19	23	7
	p	**p=0,876**		**p=0,451**		**p=0,211**	
	$CD8^+$ T-ly Median (IQ)	83,17 (33,42-94,54)	90,30 (36,29-183,00)	78,67 (27,71-115,89)	87,87 (40,48-165,44)	68,00 (33,42-155,13)	112,46 (78,67-194,67)
	n	6	28	11	23	25	9
	p	**p=0,470**		**p=0,519**		**p=0,250**	
	Ratio CD4/CD8 Median (IQ)	1,55 (1,48-1,72)	1,12 (0,91-1,78)	1,48 (0,92-1,70)	1,23 (1,00-1,78)	1,31 (1,00-1,78)	1,23 (0,97-1,55)
	n	6	24	11	19	23	7
	p	**p=0,300**		**p=0,983**		**p=0,825**	
	$CD4^+FoxP3^+$ Ly Median (IQ)	2,67 (0,00-4,00)	2,33 (0,60-8,85)	3,34 (0,45-6,17)	1,67 (0,65-7,60)	3,00 (0,65-7,25)	2,00 (0,25-15,00)
	n	6	24	11	19	23	7
	p	**p=0,500**		**p=0,829**		**p=1,000**	
	Ratio FoxP3/CD4 Median (IQ)	0,01 (0,00-0,03)	0,03 (0,01-0,06)	0,03 (0,01-0,06)	0,02 (0,01-0,06)	0,03 (0,01-0,06)	0,01 (0,01-0,07)
	n	6	24	11	19	23	7
	p	**p=0,233**		**p=0,605**		**p=0,731**	
	Total of Ly Median (IQ)	244,08 (86,11-271,43)	200,44 (100,24-322,55)	175,90 (66,57-277,70)	209,47 (115,63-284,69)	197,00 (97,27-274,03)	261,17 (201,45-371,36)
	n	6	24	11	19	23	7
	p	**p=0,717**		**p=0,355**		**p=0,230**	
	Ft Expression in EC Median (IQ)	7,50 (6,67-10,00)	10,00 (10,00-11,46)	10,00 (6,67-10,00)	10,00 (10,00-11,46)	10,00 (10,00-11,46)	10,00 (7,50-10,00)
	n	5	28	10	23	24	9
	p	**p=0,028**		**p=0,055**		**p=0,074**	
	Ft Expression in Ly Median (IQ)	8,00 (7,99-8,00)	9,00 (8,00-10,00)	10,00 (8,00-10,00)	8,00 (8,00-10,00)	8,00 (7,75-10,00)	10,00 (8,00-12,00)

	n	5	27	10	22	23	9
	p	**p=0,363**		**p=0,543**		**p=0,194**	

Abbreviations: IDC, Invasive Ductal Carcinoma; DCIS, Ductal Carcinoma *in situ*; ER, Estrogen Receptor; PR, Progesterone Receptor; HER-2, Human Epidermal Growth Factor 2; IQ, Interquartile Range; Ly, Lymphocytes; Ft, Ferritin; EC, Epithelial Cells.

Table 13 – Median ferritin expression and lymphocytic infiltration according to the clinicopathological variables for local and metastatic tumor growth in the invasive compartment.

	IDC				
Clinicopathological Variable	**Tumor Size [a]**			**Lymph Node Involvement [b]**	
	T1	T2	> T3	Negative	Positive
$CD4^+$ T-Ly Median (IQ)	137,29 (65,25-245,91)	65,11 (30,17-93,75)	142,00 (114,50-169,50)	97,95 (52,89-171,20)	93,75 (73,80-183,29)
Corr coeff. and *p*	**r=-0,314; p=0,090; n=30**			**p=0,539; n=30**	
$CD8^+$ T-Ly Median (IQ)	90,96 (55,38-213,38)	40,48 (20,33-97,27)	133,79 (112,46-155,13)	78,67 (36,71-137,22)	93,29 (36,25-171,33)
Corr coeff. and *p*	**r=-0,224; p=0,205; n=34**			**p=0,560; n=33**	
Ratio CD4/CD8 Median (IQ)	1,23 (1,01-1,78)	1,35 (0,61-1,80)	1,12 (0,74-1,51)	1,35 (0,87-1,70)	1,09 (0,99-1,78)
Corr coeff. and *p*	**r=-0,094; p=0,610; n=30**			**p=0,861; n=29**	
$CD4^+FoxP3^+$ Ly Median (IQ)	2,33 (0,63-15,10)	2,13 (0,33-4,83)	4,80 (2,00-7,00)	1,75 (0,60-5,92)	3,25 (0,33-9,50)
Corr coeff. and *p*	**r=-0,067; p=0,733; n=30**			**p=0,809; n=29**	
Ratio FoxP3/CD4 Median (IQ)	0,02 (0,00-0,06)	0,02 (0,01-0,07)	0,04 (0,01-0,06)	0,02 (0,01-0,06)	0,03 (0,01-0,06)
Corr coeff. and *p*	**r=0,005; p=0,967; n=30**			**p=0,982; n=29**	
Total of Ly Median (IQ)	239,16 (131,25-488,92)	110,43 (66,75-261,17)	280,29 276,63-283,96)	206,68 (97,21-280,29)	227,00 (97,92-352,35)
Corr coeff. and *p*	**r=-0,244; p=0,193; n=30**			**p=0,661; n=29**	
Ft Expression in EC Median (IQ)	10,00 (10,00-10,83)	10,00 (7,50-11,04)	constant	10,00 (7,50-10,83)	10,00 (10,00-11,25)
Corr coeff. and *p*	**r=-0,072; p=0,693; n=33**			**p=0,748; n=32**	
Ft Expression in Ly Median (IQ)	9,00 (8,00-10,00)	8,00 (7,67-10,00)	9,00 (8,00-10,00)	8,00 (7,33-10,00)	8,50 (8,00-10,00)
Corr coeff. and *p*	**r=-0,069; p=0,699; n=32**			**p=0,597; n=32**	

[a]: The Spearman's rank correlation coefficient was used to evaluate the relationship between variables.
[b]: Mann-Whitney test was applied to evaluate the association between categorical variables.

Abbreviations: Correlation coefficient, Corr coeff.; IDC, Invasive Ductal Carcinoma; IQ, Interquartile Range; Ly, Lymphocytes; Ft, Ferritin; EC, Epithelial Cells.

Ferritin Expression in Breast Cancer Infiltrating Lymphocytes

Leite, Luciana, BSc[1]; Marques, Oriana, MSc[1,2,3,4]; Rosa, Ana, BSc[1,3,4]; Rêma, Alexandra, BSc[1]; Faria, Fátima, BSc[1]; Porto, Graça, MD, PhD[1,3,4,5]; Cruz Paula, Arnaud, MSc[2,6]; Lopes, Carlos, MD, PhD[1,6]; Martins da Silva, Berta, PhD[1,2]

1 - Pathology and Molecular Immunology Department, Institute of Biomedical Sciences Abel Salazar (ICBAS), University of Porto, Porto, Portugal;
2 - Unit for Multidisciplinary Biomedical Research (UMIB), Institute of Biomedical Sciences Abel Salazar (ICBAS), University of Porto, Porto, Portugal;
3 - Basic and Clinical Research on Iron Biology, Instituto de Biologia Molecular e Celular (IBMC), University of Porto, Porto, Portugal
4 - Instituto de Investigação e Inovação em Saúde (i3S), University of Porto, Porto, Portugal;
5 - Hematology Service, Hospital de Santo António, Centro Hospitalar do Porto, Porto, Portugal;
6 - Department of Pathology, Portuguese Oncology Institute (IPO), Porto, Portugal

Background

It is well accepted that breast cancer is characterized by a **deregulation** in cellular iron homeostasis, as revealed by differences in the expression of several iron-related proteins, relating with markers of poor outcome. Accumulating evidence has shown that distribution and function of **T-lymphocytes** could be altered, enhancing immune surveillance of cancer cells. Previous studies showed that lymphocytes are capable of **ferritin** synthesis and secretion. Data from our group reported that ferritin was overexpressed in lymphocytes from breast ductal carcinoma samples. We also observed an increased hemosiderin deposition in these samples, suggesting that lymphocytes and macrophages might constitute an effective iron "reservoir".

The **main objective** of this work was to verify if a certain "immune-profile" is related to a higher/lower expression of ferritin. More specifically, we proposed to analyze if lymphocyte numbers and ferritin expression were influencing clinicopathological variables of breast cancer progression and behaviour.

Material & Methods

Lymphocyte numbers (CD4, CD8 and FoxP3) and ferritin expression were assessed by immunohistochemistry in 134 tissue microarray spots, consisting of 86 primary samples (34 invasive ductal carcinomas (IDC), 27 ductal carcinomas *in situ* (DCIS) and 25 breast reduction samples as controls). Ferritin expression in the epithelium and leukocyte infiltrate was evaluated by a semi-quantitative method, considering the stained area and its intensity. The total number of lymphocytes was assessed in 5 High-Power Fields (400x). Hemosiderin deposits in epithelial and stromal inflammatory cells were detected with the DAB-enhanced Perls' staining.

Results

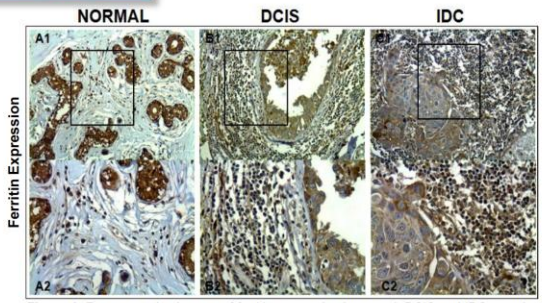

Figure 1: Representative images of ferritin expression in normal, DCIS and IDC samples. Original magnification (A1-B1-C1) 200x and (A2-B2-C2) 400x.

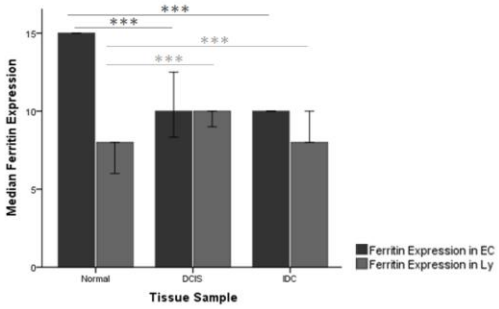

Figure 2: Ferritin expression in epithelial cells (EC) and lymphocytes (Ly) from normal, DCIS and IDC samples. Graph shows Median and 95% Confidence Interval (CI). Significant differences are shown for comparison with the precedent group *p<0,05; **p<0,01; ***p<0,001, Mann-Whitney test.

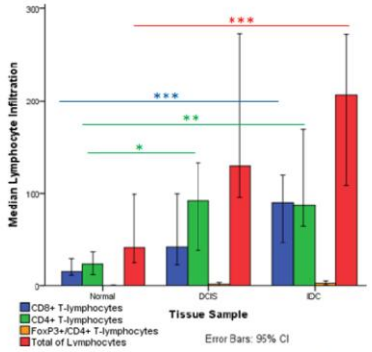

Figure 3: Ly frequencies in breast tissue samples. Graph shows Median and 95% CI. Significant differences are shown for comparison with the precedent group *p<0,05; **p<0,01; ***p<0,001, Mann-Whitney test.

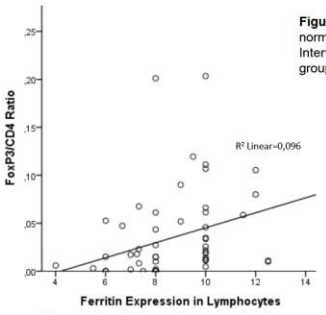

Figure 4: Scatter diagram of Spearman correlation coefficient between FoxP3/CD4 ratio and ferritin expression in Ly.

Table 1: Influence of hemosiderin deposition in stromal inflammatory cells on ferritin expression (IQ, Interquartile Range).

	Hemosiderin Deposition in Stromal Inflammatory Cells			
	Absence		Presence	
Ferritin Expression	n	Median (IQ)	n	Median (IQ)
Epithelial Cells	29	10,00 (10,00-15,00)	37	10,00 (7,50-12,50)
p	p=0,018			
Lymphocytes	22	9,25 (7,33-10,00)	33	8,00 (8,00-10,00)
p	p=0,958			

Conclusions

- Breast cancer EC presented a significantly **lower** expression of ferritin than normal samples (p<0,001). In breast cancer infiltrating lymphocytes, ferritin expression was significantly **higher** compared to normal samples (p<0,001) (Figure 2);
- The total of lymphocyte population was much **more pronounced** in carcinoma (DCIS and IDC) than in control normal samples (p<0,05) (Figure 3);
- FoxP3/CD4 ratio was positively **correlated** with ferritin expression in lymphocytes (p=0,002), evidencing the importance of ferritin in regulatory T-cells induction (Figure 4);
- CD4/CD8 ratio was not correlated with ferritin expression in lymphocytes (p>0,05) (Data not shown);
- Ferritin expression in lymphocytes **was not correlated** with iron accumulation in stromal inflammatory cells (p=0,958), indicating that increased infiltration of ferritin-rich lymphocytes in breast tumors may play a role not yet unraveled (Table 1);
- The release of ferritin by lymphocytes may favor breast cancer progression, not only by acting as an **immunosuppressive effector**, but also as an **alternative** route of iron delivery to tumor cells.

References: Dorner M.H. et al. (1980) Science 209: 1019;
Alkhateeb A. et al. (2013) Breast Cancer Res Treat 137: 733;
Marques O. et al. (2014) Annals of Oncology 25, supp 1: i18.

Acknowledgements: